Received: 19 May 2021 | Revised: 6 December 2021 | Accepted: 6 December 2021

DOI: 10.1111/joa.13614

Journal of Anatomy ANATOMICAL SOCIETY WILEY

ORIGINAL PAPER

Musculotendinous system of mesopelagic fishes: Stomiiformes (Teleostei)

Nalani K. Schnell[1] | Jürgen Kriwet[2] | Faviel A. López-Romero[2] | Guillaume Lecointre[3] | Cathrin Pfaff[2]

[1]Institut Systématique, Evolution, Biodiversité (ISYEB), Muséum National d'Histoire Naturelle, CNRS, SU, EPHE, UA, Concarneau, France

[2]Department of Palaeontology, University of Vienna, Vienna, Austria

[3]Institut Systématique, Evolution, Biodiversité (ISYEB), Muséum national d'Histoire naturelle, CNRS, SU, EPHE, UA, Paris, France

Correspondence
Nalani K. Schnell, Institut Systématique, Evolution, Biodiversité (ISYEB), Muséum national d'Histoire naturelle, CNRS, SU, EPHE, UA, Station Marine de Concarneau, Place de la Croix, 29900 Concarneau, France.
Email: nalani.schnell@mnhn.fr

Funding information
This project was funded by OEAD Amandée (FR 09/2016) and PHC Amadeus 2016 Project n° 35565YE.

Abstract

Every night the greatest migration on Earth starts in the deep pelagic oceans where organisms move up to the meso- and epipelagic to find food and return to the deeper zones during the day. One of the dominant fish taxa undertaking vertical migrations are the dragonfishes (Stomiiformes). However, the functional aspects of locomotion and the architecture of the musculotendinous system (MTS) in these fishes have never been examined. In general, the MTS is organized in segmented blocks of specific three-dimensional 'W-shaped' foldings, the myomeres, separated by thin sheets of connective tissue, the myosepta. Within a myoseptum characteristic intermuscular bones or tendons may be developed. Together with the fins, the MTS forms the functional unit for locomotion in fishes. For this study, microdissections of cleared and double stained specimens of seven stomiiform species (*Astronesthes* sp., *Chauliodus sloani*, *Malacosteus australis*, *Eustomias simplex*, *Polymetme* sp., *Sigmops elongatus*, *Argyropelecus affinis*) were conducted to investigate their MTS. Soft tissue was investigated non-invasively in *E. schmidti* using a micro-CT scan of one specimen stained with iodine. Additionally, classical histological serial sections were consulted. The investigated stomiiforms are characterized by the absence of anterior cones in the anteriormost myosepta. These cones are developed in myosepta at the level of the dorsal fin and elongate gradually in more posterior myosepta. In all but one investigated stomiiform taxon the horizontal septum is reduced. The amount of connective tissue in the myosepta is very low anteriorly, but increases gradually with body length. Red musculature overlies laterally the white musculature and exhibits strong tendons in each myomere within the muscle bundles dorsal and ventral to the horizontal midline. The amount of red musculature increases immensely towards the caudal fin. The elongated lateral tendons of the posterior body segments attach in a highly complex pattern on the caudal-fin rays, which indicates that the posterior most myosepta are equipped for a multisegmental force transmission towards the caudal fin. This unique anatomical condition might be essential for steady swimming during diel vertical migrations, when prey is rarely available.

KEYWORDS

Argyropelecus, *Astronesthes*, caudal fin, *Chauliodus*, comparative anatomy, deep-sea fishes, diel vertical migration, dragonfishes, *Eustomias*, functional morphology, Gonostomatidae, intermuscular bones, locomotion, *Malacosteus*, myosepta, Phosichthyidae, *Polymetme*, red musculature, *Sigmops*, Sternoptychidae, Stomiidae

1 | INTRODUCTION

Micronektivore fishes of the oceanic mesopelagic zone (between 200 and 1000 m), like Stomiiformes and Myctophiformes, migrate to the epipelagic layer (0–200 m depth) in order to feed on other migrating micronektonic fishes, shrimps, and/or cephalopods (e.g., Brierley, 2014; Sutton & Hopkins, 1996; Sutton et al., 2010). These diel vertical migrations (DVM) play an important role in the world carbon cycle (Eduardo et al., 2020; Martin et al., 2020) and, therefore, in the world's climate. Ecologically this means that such micronektivores are trophic mediators linking surface waters to those of their deeper daytime depth ranges (Marks et al., 2020; Sutton & Hopkins, 1996). Even though we still do not know much about these zones, recent advances in deep-sea surveys have provided a glimpse into this world of extremes, its vertical connectivity of the food webs between the epipelagic and deeper zones (Badcock, 1970; Drazen & Sutton, 2017) and the swimming behaviour of its inhabitants (Bailey et al., 2003, 2005; Sward et al., 2019).

Many stomiid fish species are impressive piscivorous predators exhibiting elongate, snake-like black bodies and large mouths with extremely large teeth. The stomiid assemblage in the Gulf of Mexico, e.g., regularly undertakes migrations from the lower mesopelagic to the epipelagic zone (Sutton, 2013; Sutton & Hopkins, 1996). Exceptions from the regular DVM pattern are the semi-migratory (e.g., *Photostomias guernei*, *Stomias affinis*, *Chauliodus sloani*) and the non-migratory species (e.g., *Malacosteus niger*). It is presumed that some taxa (e.g. *Chauliodus*, *Stomias*) position themselves at the main depth of upward and downward migration to find and ambush their prey (Sutton & Hopkins, 1996). The almost neutrally buoyant mesopelagic fishes are able to undertake DVMs due to their large proportions of red muscle fibres, which were investigated with transverse sections through the tail in several species (Marshall, 1971). Red muscle fibres are, in contrast to white muscle fibres, rich in fat and contain a lot of glycogen, myoglobin, mitochondria, and are highly vascularized (e.g., Boddeke et al., 1959). However, the functional aspects of locomotion and the architecture of the musculotendinous system (MTS) have never been investigated in detail in mesopelagic fishes.

The MTS of the trunk of fishes forms together with their fins the functional unit of locomotion (e.g. Alexander, 1967; Breder, 1926; Gray, 1933a, 1933b, 1933c; Lauder, 2015; Videler, 1993). This system is organized in segmental blocks of specific three-dimensional 'W'-shaped muscle blocks, the myomeres. Adjacent myomeres are separated by thin sheets of connective tissue, the myosepta, which can be additionally characterized by ossified tendons, also known as intermuscular bones (e.g. Danos et al., 2008; Gemballa & Röder, 2004; Patterson & Johnson, 1995). This MTS is well investigated in shallow water fishes (e.g. Danos et al., 2008; Gemballa et al., 2006; Gemballa & Röder, 2004; Schwarz et al., 2012) and is highly conservative in its anatomy among gnathostome fishes (Gemballa, Ebmeyer, et al., 2003; Shadwick & Gemballa, 2006).

However, anatomical investigations of different ecological fish types inhabiting the upper 200 m of the oceans indicate morphological differences in the MTS and their respective swimming mode (e.g. Schwarz et al., 2012; Shadwick & Gemballa, 2006). Fast swimming predators of the open ocean (e.g., tunas and sharks) are characterized by stiff bodies that display only slight body curvatures during swimming (e.g., Gemballa et al., 2006), whereas flexible, elongated fishes like eels undergo extreme body curvatures during swimming in a more complex habitat (e.g. Danos et al., 2008; Schwarz et al., 2012). These differences in the swimming mode are reflected in the shape of the MTS and the amount of red musculature (Danos et al., 2008). Besides myoseptal tendon length and distribution of white and red muscle packages, the attachment line of myosepta on the vertebral axis also differs extensively between flexible and rigid fishes (Schwarz et al., 2012; Shadwick & Gemballa, 2006). In flexible fishes, the attachment line crosses two or three vertebral segments along the neural arches and then connects to the neural spine. In contrast, the attachment line in rigid fishes remains within one vertebral centrum and follows the neural spine of the same segment (Shadwick & Gemballa, 2006). As a consequence, rigid fishes possess a transmission of muscle force from the anterior region of the body to the tail region and can generate high speeds in contrast to flexible fishes of the upper ocean zones.

Here, we address this gap in our knowledge of the morphology of the MTS in stomiiform fishes inhabiting the meso- and bathypelagic and highlight anatomical differences between diel vertical migrators and non-migrators. Thus, we provide, for the first time, a detailed anatomical description of the MTS of Stomiiformes.

2 | METHODS

During this study, specimens of eight species representing four stomiiform families were investigated (Table 1). Studied specimens were obtained on loan from the ichthyological collections of the Museum of Comparative Zoology (MCZ), Harvard University, Cambridge, Massachusetts, USA; Muséum national d'Histoire naturelle (MNHN), Paris, France; Natural History Museum (BMNH), London, UK; National Museum of Natural History (USNM), Smithsonian Institution, Washington DC, USA, and Scripps Museum of Oceanography (SIO), San Diego, USA.

For microdissection of myosepta, specimens were cleared and double stained (C&S) according to protocols of Dingerkus and Uhler (1977) and Taylor and van Dyke (1985). Microdissections were carried out to analyse and visualize the morphology of the myosepta and their collagen fibre tracks. The C&S specimens subsequently were transferred stepwise into ethanol (final: solution of 96%) to better visualize the connective tissue. The collagen tracks and tendons within the myosepta were examined under polarized light with a polarization filter. The axial position of every myoseptum is defined as the anterior-most position of its insertion line on the vertebral column (axial position 0,0*L* represents the tip of the snout; 1,0*L* represents the tip of the caudal fin). Due to anatomical differences of myosepta between body regions, we decided to dissect and measure different distances (see data analyses) and photograph all myosepta of every specimen. Each myoseptum on the right side of

TABLE 1 List of species investigated for this study

Taxon	Collection number	SL (mm)	n° specimens	Method	Migration types
Gonostomatidae					
Sigmops elongatus	MNHN 2003 1394	175	1	C&S	Migratory[a,b,e] Non-migratory[d]
Cyclothone atraria	SIO 67-102	TL = 68	1	Histo	
Sternoptychidae					
Argyropelecus affinis	MNHN 2021-0224	59	1	C&S	Short diel migrations or non-migratory[a,f]
Argyropelecus olfersii	MNHN 2021-0223	62	1	C&S	
Phosichthyidae					
Polymetme sp.	MNHN 1997 830	160	1	C&S	Non-Migratory[a] Migratory[g]
Stomiidae					
Astronesthes sp.	MNHN 2000 0576	131	1	C&S	Migratory[a]
Astronesthes leucopogon	USNM 35907	118	1	C&S	
Astronesthes niger	MCZ 133101	62	1	Histo	
Borostomias elucens	USNM uncatalogued	ca. 110	1	Ethanol preserved	
Stomias affinis	USNM 358765	114	1	Ethanol preserved	
Chauliodus barbatus	USNM 394241	188	1	C&S	
Chauliodus sloani	MNHN 2021-0225	264	1	C&S	Semi-Migratory[c,h] Migratory[b,h]
Chauliodus sloani	USNM 200984	145	1	C&S	
Chauliodus sloani	MCZ 157964	TL = 138	1	Histo	
Idiacanthus atlanticus	USNM 206705	327	1	Ethanol preserved	
Eustomias filifer	BMNH 2007.10.31.12	TL = 97	1	Histo	
Eustomias obscurus	USNM 206711	199	2	C&S	Migratory[a]
Eustomias schmidti	USNM 261301	185	1	Iodine staining CT scan	Migratory[a] with non-diel periodicity[c]
Eustomias simplex	USNM 372020	223	1	C&S	Migratory[a]
Malacosteus australis	USNM 296675	110	1	C&S	Non-Migratory[i]
Malacosteus australis	SIO 73-25	TL = 100	1	Histo	
Malacosteus australis	SIO 73-25	TL = 135	1	Ethanol preserved	

Abbreviations: MCZ, Museum of Comparative Zoology; Harvard, USA; MNHN, Muséum national d'Histoire naturelle, Paris, France; SIO, Scripps Museum of Oceanography, San Diego, USA; USNM, Smithsonian National Museum of National History, Washington, USA.

[a]Badcock (1984)
[b]Woodstock (2018)
[c]Sutton and Hopkins (1996)
[d]Wienerroither et al. (2009)
[e]Richards et al. (2020)
[f]Kinzer and Schulz (1988)
[g]Cornejo and Koppelmann (2006)
[h]Eduardo et al. (2020)
[i]Kenaley (2007).

the specimen was removed in toto and placed under a Zeiss SteREO Discovery.V20. For this, each myoseptum was spread on a microscopic slide or petri dish in 96% ethanol and then photographed under polarized light (see also Gemballa & Britz, 1998). Collagenous fibres and tendons of a myoseptum appear bright white, mineralizations in pink or red, whereas the remaining parts of a myoseptum are in black. Images were taken with a Zeiss Axiocam attached to the Zeiss SteREO Discovery.V20. Figures were created with Adobe Illustrator CS6.

Soft tissue was investigated non-invasively in one iodine-stained specimen of *Eustomias schmidti* using micro-CT scans, following the protocol of Metscher (2009). The micro-CT scan (Skyscan/Bruker 1173) was carried out at the Department of Palaeontology at the University of Vienna. Scan settings were as following: scan

resolution: 15.02 μm; voltage: 50 kV, 160 μA; frame averaging of three. The 3D dataset was visualized with DataViewer 1.5.4.0 (Skyscan/Bruker) and Amira 6.1.1. (Thermo Fisher Scientific).

Histological serial sections were embedded in Paraffin and stained with Azan after Domagk (1933).

For the data analyses, statistical tests were carried out to investigate differences between species and migration groups with four different tendon-measurements of the seven examined taxa (Tables 1–8): MTep, MThyp: length of the epaxial (dorsal) and hypaxial (ventral) myorhabdoid tendon (MT); LTep, LThyp: length of the epaxial and hypaxial lateral tendon (LT), which corresponds to the distance between anterior and posterior cone (detailed measurements see Table S1).

The tendon length was adjusted as percentages of the standard length of each individual. To check if the data were normally distributed, we first applied a 'Shapiro–Wilk test' to each one of the four measurements (Table 2). Since the trait data indicated no normal distribution, the subsequent analyses were performed with non-parametric tests. First, we applied a 'Kruskal–Wallis test' to assess the differences of each trait among species (Table 3) and groups (migratory, non-migratory and semi-migratory). This was done both considering *Eustomias* as part of the migratory group (migratory species according to Sutton & Hopkins, 1996) (Table 4) and excluding *Eustomias* from the analyses (Table 7), as its MTS highly resembles that of the non-migratory species *Malacosteus australis*. If the test indicated differences between the groups, we conducted a 'pairwise Wilcoxon rank sum test' with Bonferroni corrections for multiple comparisons for the differences between species (Table 5), between groups with *Eustomias* in the migratory group (Table 6), and between groups excluding *Eustomias* (Table 8). All the tests were carried out with base functions in R 3.6.3 (R Core Team, 2020). Plots were produced with ggplot2 (Wickham, 2016) and viridisLite (Garnier, 2018).

Trees as a way to explore constraints. From the present anatomical description, we aimed to detect whether functional convergences could distort the phylogenetic relationships of the present taxa as depicted by Kenaley et al. (2013). We searched for characters that showed different character states across taxa; this resulted in a matrix of 18 characters (Table 9), of which 14 are parsimony informative (i.e. showing at least two states, each present at least twice across taxa). Characters 3, 6, 17 and 18 are interesting from an anatomical point of view, but of little significance for tree search.

A hierarchical graph of maximum consistency (i.e. maximum parsimony) was calculated using the exhaustive search of PAUP* (Swofford, 2002, characters unweighted and unordered) in order to compare it with the interrelationships of our present taxa obtained by pruning the tree of Kenaley et al. (2013). According to that study, where *Sigmops elongatus* is together with *Vinciguerria* sister to all other taxa, our tree was rooted on *S. elongatus*.

TABLE 2 Shapiro–Wilk normality test for each of the measured traits

Trait	W	*p*
LTep	0.95309	**1.909e−05**
MTep	0.94842	**6.126e−06**
LThyp	0.96055	**0.0001636**
MThyp	0.93865	**2.239e−05**

Note: Bold indicates $p < 0.05$.

Abbreviations: LTep, lateral tendon epaxial; LThyp, lateral tendon hypaxial; MTep, myorhabdoid tendon epaxial; MThyp, myorhabdoid tendon hypaxial.

2.1 | 3D-shape and architecture of myosepta

Myosepta separate adjacent myomeres and exhibit a 'W'-shape when observed in lateral view (Figure 1a). The horizontal septum (when present) separates the dorsal epaxial and ventral hypaxial parts along the horizontal midline. A myoseptum is characterized by four cones and two areas connecting these (Figure 1a). The same cones of successive myosepta are nested within each other. The dorsal anterior cone (DAC) and the dorsal posterior cone (DPC) are connected by the epaxial sloping part (ESP). The ventral anterior cone (VAC) and the ventral posterior cone (VPC) are connected by the hypaxial sloping part (HSP) (e.g. Gemballa & Britz, 1998; Gemballa & Röder, 2004). In this study, the anterior cone refers to the anterior elongation of the myoseptum that lies in front of the anterior border of the centrum that the myoseptum attaches to, the posterior cone refers to the elongation of the myoseptum that lies posterior to the hind margin of the centrum that the myoseptum attaches to. The part of the myoseptum that lies between the anterior and posterior border of the centrum is called the sloping part; however, the transition from cones to sloping parts is not distinct. These landmarks are useful to measure the anterior or posterior elongation of the cones.

Different collagen fibre tracts are visible in the epaxial and hypaxial parts of the myoseptum (Figure 1b). Distinct collagen fibre tracts of the LT lie in the ESP connecting the DAC and DPC, and also in the HSP connecting the VAC and VPC. In the ESP and HSP, the LT can be intersected by the epineural tendon (ENT) epaxially, and by the epipleural tendon (EPT) hypaxially with both these tendons running caudolaterally towards the skin. The entire flanking parts, epaxially and hypaxially of each myoseptum, are invested by fibre tracts of the MT.

2.2 | Controversy about intermuscular bones

Intermuscular bones only occur in teleosts amongst recent vertebrates and are serially arranged ossifications in the myosepta (e.g. Gemballa, Ebmeyer, et al., 2003; Owen, 1846, 1866; Patterson & Johnson, 1995) (Figure 1c–e). The three principal series of recognized intermusculars are the epineurals, epicentrals and the epipleurals (Gemballa, Ebmeyer, et al., 2003; Owen, 1846; Patterson & Johnson, 1995). It has been suggested that

TABLE 3 Kruskal–Wallis test results. Four traits analysed for all species

Trait	Df	χ^2	*p*
LTep	7	143.15	**<2.2e−16**
MTep	7	108.52	**<2.2e−16**
LThyp	7	131.12	**<2.2e−16**
MThyp	7	105.85	**<2.2e−16**

Note: Bold indicates $p < 0.05$.

Abbreviations: LTep, lateral tendon epaxial; LThyp, lateral tendon hypaxial; MTep, myorhabdoid tendon epaxial; MThyp, myorhabdoid tendon hypaxial.

TABLE 4 Kruskal–Wallis test results. Differences between the groups (migratory, semi-migratory and non-migratory) for all investigated traits

	df	χ^2	*p*
LTep	2	12.694	**0.001752**
MTep	2	7.8007	**0.02023**
LThyp	2	9.202	**0.01004**
MThyp	2	11.214	**0.003671**

Note: Bold indicates $p < 0.05$.

they reinforce and stabilize myosepta (Van Leeuwen, 1999; Wainwright, 1983) and further possibly transmit muscular forces from myomeres to the axial skeleton (Danos & Ward, 2012; Gemballa, Ebmeyer, et al., 2003).

However, questions on the terminology, homology and function of intermuscular bones and their tendinous/ligamentous precursors are still not fully resolved. Gemballa and Britz (1998) used the term 'intermuscular tendons' (epineural tendon, ENT; epicentral tendon, ECT; epipleural tendon, EPT) instead of 'intermuscular ligaments' (Patterson & Johnson, 1995), with the explanation that tendons connect muscle to bone, whereas ligaments connect bone to bone. Additionally, Gemballa and Britz (1998) explain that 'intermuscular tendons' transfer muscular forces from myomeres to the axial skeleton and thus act as tendons. In their response, Johnson and Patterson (2001) stated that the transmission of force has not been proven and changing the terminology of an already complicated system like the 'intermuscular ligaments' will not help in future communications. Keeping this in mind we herein decided to maintain the term 'intermuscular tendons' (Gemballa & Britz, 1998) as literature about functional morphology of the MTS applies this terminology (e.g. Danos et al., 2008; Schwarz et al., 2012; Shadwick & Gemballa, 2006; Westneat et al., 1993).

Further necessary information on the terms epineural/epipleural: The ossification referred to as 'epineural'/'epipleural' can be located within the ENT/EPT and/or the LT (a tendon overlooked in most anatomical studies). Usually within the epaxial part of the myoseptum (we only refer to the epaxial part here, however, the same is true for the hypaxial part) two fibre-bundles can be recognized. (1) The ENT (epineural ligament of Patterson & Johnson, 1995) originates on the neural arch and extends posterolaterally towards the skin. (2) The LT originates in the DAC and runs dorsolaterally into the posterior dorsal cone. An ossification can be variably found in either of the two fibre bundles (Figure 1c,e), in both or in none of them. If an ossification is present in both structures, this results in a proximally forked ossification (Figure 1d) also previously called 'epineural' in anatomical studies, as there has been no distinction between the three ossification patterns of the bone situated in ENT, in LT or in ENT+LT (e.g. *Gonorhynchus*; Patterson & Johnson, 1995). This proximally forked ossification has a primary anteromedial branch attaching it to the neural arch or spine and a secondary anteroventral branch passing to the transverse process of the preceding vertebra without attaching to the vertebral column (Patterson & Johnson, 1995, p. 7). In the intermuscular tables of Patterson and Johnson (1995), the LTB was coded with the symbol 'V' ('epineural bone, a member of a series with anteroventral branching, in which the medial branch attaching to the axial skeleton is lost, so that the remaining part represents only the anteroventral branch and the posterior part of the bone'; p. 50). However, the presence/absence of only the tendon (ENT/LT) without ossification was not taken into account in their table. We here consider it critical to note presence/absence of an ENT/LT as well as to differentiate between the three different ossification patterns within these tendons. In order to avoid changing an existing terminology, we decided to keep the term epineural bone (ENB) as an umbrella term for either of the ossifications, with an additional distinction if the ossification lies within the epineural tendon (ENTB) or in the lateral tendon (LTB) or in both. Difficulties only arise regarding the identity of the posterior part of the ossification that extends into the posterior cone; it appears as if the fibre bundles of the epineural and LT merge posteriorly (Figure 1b; see also Gemballa, Ebmeyer, et al., 2003, Figure 4). Further studies are necessary to completely understand the different ossification patters for epineural/epipleural bones.

2.3 | List of Abbreviations

The herein applied terminology to describe the anatomy of a myoseptum is based on the terminology introduced by Alexander (1969) and modified by Gemballa, Ebmeyer, et al. (2003): DAC, dorsal anterior cone; DPC, dorsal posterior cone; ECT, epicentral tendon (synonym of AOT, anterior oblique tendon, see e.g. Kafuku, 1950 or Patterson & Johnson, 1995 for discussion); EFP, epaxial flanking part; ENB, epineural bone (umbrella term; explanation see above); ENT, epineural tendon; ENTB, epineural tendon bone; EPB, epipleural bone (umbrella term; explanation see above); EPT, epipleural tendon; EPTB, epipleural tendon bone; ESP, epaxial sloping part; F.NL, foramen for the *nervus lateralis*; HM, horizontal midline; HS, horizontal septum; HSP, hypaxial sloping part; LT, lateral tendon; LTB, lateral tendon bone; LTu, lateral tendon of compound ural centrum; MT, myorhabdoid tendon; MTS, musculotendinous system; R, rib; RM, red musculature; RMA, attachment site of red musculature; RMT, tendon within red muscle bundles; V, vertebra; VAC, ventral anterior cone; VPC, ventral posterior cone; VSAC, ventral secondary anterior cone.

TABLE 5 Wilcoxon pairwise comparison of the traits between species, *p* values after Bonferroni corrections

	Arg_aff	Astr_sp	Cha_slo	Eus_obs	Eus_sim	Mal_aus	Poly_sp
LTep							
Astr_sp	1						
Cha_slo	**9.4e−05**	**0.00011**					
Eus_obs	**7.7e−12**	**1.6e−05**	**3.1e−11**				
Eus_sim	**6.5e−07**	**0.00102**	**5.5e−06**	1			
Mal_aus	**6.7e−09**	**9.2e−05**	**6.1e−06**	**0.00489**	**0.00022**		
Poly_sp	**0.0023**	0.28025	**1.9e−07**	**3.0e−12**	**4.0e−07**	**8.1e−10**	
Sig_elo	1	1	**6.7e−06**	**3.0e−12**	**4.0e−07**	**8.1e−10**	1
MTep							
Astr_sp	1						
Cha_slo	1	1					
Eus_obs	**2.3e−10**	**9.6e−08**	**1.1e−12**				
Eus_sim	**2.7e−07**	**1.1e−05**	**2.2e−09**	1			
Mal_aus	**0.00631**	**0.0253**	0.1215	1	0.3904		
Poly_sp	0.09415	0.39574	**0.00226**	**1.5e−07**	**6.6e−05**	**0.00014**	
Sig_elo	0.3363	0.88781	**0.00367**	**3.0e−12**	**1.6e−07**	**3.4e−05**	1
LThyp							
Astr_sp	0.32474						
Cha_slo	**0.03608**	**0.00011**					
Eus_obs	**2.1e−07**	**1.4e−05**	**1.4e−11**				
Eus_sim	**1.2e−05**	**1.1e−05**	**5.0e−05**	1			
Mal_aus	**8.6e−05**	**1.1e−05**	**0.00154**	**0.01118**	1		
Poly_sp	**0.00011**	0.145781	**2.2e−07**	**1.2e−07**	**3.2e−07**	**1.5e−08**	
Sig_elo	1	1	**0.00635**	**1.2e−07**	**4.8e−06**	**9.4e−06**	1
MThyp							
Astr_sp	**0.00355**						
Cha_slo	1	**0.00277**					
Eus_obs	**2.6e−05**	**1.4e−08**	**8.8e−07**				
Eus_sim	**0.00049**	**2.1e−05**	**4.1e−05**	1			
Mal_aus	**0.0001**	**1.1e−06**	**1.0e−05**	1	1		
Poly_sp	**0.00022**	1	**1.7e−05**	**2.1e−10**	**1.8e−06**	**4.8e−08**	
Sig_elo	**0.00018**	1	**0.00178**	**1.1e−06**	**0.00019**	**2.0e−05**	1

Note: Bold indicates $p < 0.05$.

Taxa: Arg_aff, *Argyropelecus affinis*; Astr_sp, *Astronesthes* sp.; Cha_slo, *Chauliodus sloani*; Eus_obs, *Eustomias obscurus*; Eus_sim, *Eustomias simplex*; Sig_elo, *Sigmops elongatus*; Mal_aus, *Malacosteus australis*. Traits: LTep, lateral tendon epaxial; LThyp, lateral tendon hypaxial; MTep, myorhabdoid tendon epaxial; MThyp, myorhabdoid tendon hypaxial.

3 | RESULTS

3.1 | *Astronesthes* sp. (MNHN 2000 0567)

3.1.1 | Myosepta

In all body regions, the myosepta span about four centra (Figure 2a–e). The anteriormost myosepta (V1–V31) exhibit a tiny DAC that reaches the anterior border of its corresponding centrum, as well as a small DPC (Figure 2a,b,e). The DAC elongates gradually, beginning on V26. At its maximal anterior elongation (V46–V51), it extends to the anterior border of its preceding centrum (Figure 2c). The dorsal and ventral anterior cones are widely separated in the caudal region. This is due to a higher number of overlapping anterior cones in this region and the increasing extent of red musculature. This is found in all investigated taxa and only stated once under *Astronesthes* sp. (e.g., Figures 2d and 6e).

3.1.2 | Intermuscular tendons and bones

ECT—The myosepta of V1–V36 have an ECT, which is distally forked (Figures 3a and 4a–c). It inserts below the midline on the ventral half

TABLE 6 Wilcoxon pairwise comparison of the traits between the groups, p values after Bonferroni corrections

	Migratory	Non-migratory
LTep		
Non-migratory	**0.035**	
Semi-Migratory	0.496	**6.6e−07**
MTep		
Non-migratory	0.0909	
Semi-Migratory	1	**0.0013**
LThyp		
Non-migratory	0.05239	
Semi-Migratory	1	**0.00017**
MThyp		
Non-migratory	**0.0093**	
Semi-Migratory	1	**1.1e−06**

Note: Bold indicates $p < 0.05$.

Migratory = *Argyropelecus affinis*, *Eustomias obscurus*, *Eustomias simplex*, *Astronesthes* sp., *Sigmops elongatus*, *Polymetme* sp.; Semi-Mig = *Chauliodus sloani*; Non-Mig = *Malacosteus australis*

TABLE 8 Wilcoxon pairwise comparison of the traits between the groups, *p* values after Bonferroni corrections

	Migratory	Non-Migratory
LTep		
Non-Migratory	**4.6E−11**	
Semi-Migratory	**3.5E−13**	**6.6E−07**
MTep		
Non-Migratory	**4.1E−09**	
Semi-Migratory	**8.1E−10**	**0.00017**
LThyp		
Non-Migratory	**5.6E−07**	
Semi-Migratory	**0.0011**	**0.0013**
MTep		
Non-Migratory	**1.5E−09**	
Semi-Migratory	**0.00096**	**1.1E−06**

Note: Bold indicates $p < 0.05$.

Migratory = Argyropelecus *affinis*, *Astronesthes* sp., *Sigmops elongatus*, *Polymetme* sp.; Semi-Mig = Chauliodus *sloani*; Non-Mig = Malacosteus *australis*.

TABLE 7 Kruskal–Wallis test results. Differences between the groups (migratory, semi-migratory and non-migratory) for all investigated traits. Excluding both *Eustomias* species from the data set

Trait	df	χ^2	*p*
LTep	2	86.073	**<2.2e−16**
MTep	2	64.527	**9.73E−015**
LThyp	2	35.405	**2.05E−08**
MThyp	2	48.574	**2.83E−11**

Note: Bold indicates $p < 0.05$.

TABLE 9 Data matrix

Astronesthes sp.	000000111100101002
Chauliodus sloani	111010010101101101
Eustomias simplex	112121- - - 010010000
Malacosteus australis	101120010010010100
Sigmops elongatus	101030101110110000
Polymetme sp.	001030101110110000
Argyropelecus affinis	101030000111110010

Characters (18 columns numbered from left to right) listed in text and taken exclusively from presented anatomical description. Bar means 'non applicable'.

of the centrum, runs along the dorsal margin of the foramen for the *nervus lateralis* and further into the DPC (Figures 3a and 4b). Additional fibres with a ventrally mirrored course of the ECT are present, which end below the foramen for the *n. lateralis*. Starting from V32, the ECT of succeeding myosepta shortens and it no longer extends into the DPC, but inserts on the midline of the centrum (Figures 2a,b and 3b,c).

ENB/EPB—In the myosepta of V1–V28, a simple ENB is present and attaches tendinously to the neural arch (ossification in the ENT; Figures 3a,b and 4a). In the myosepta of V29–V32, the ossification is proximally forked (ossification in the ENT+LT; Figure 3c). The same is true for the EPBs in the hypaxial part of the myoseptum; however, the proximally forked EPBs are present further posteriorly in the myosepta of V31–V36 (Figures 2b,e and 3c). The antero-medial branch of the forked intermuscular is still attached to the neural arch (parapophysis respectively) and represents the ossification in the ENT (EPT respectively), whereas the anterolateral branch of the forked bony element is an ossification in the LT. Further posteriorly the epineural and epipleural ossifications are absent, but the tendons (ENT, EPT) are present up to V37. In myosepta of V33 epaxially and V37 hypaxially up to V53, the simple ENB is an ossification in the LT and spans between the anterior and posterior cones (Figure 3e).

MT—A MT is present dorsally and ventrally in all investigated body regions (Figure 2a–e). Anterior to V24 the ventral MT is missing.

3.1.3 | Horizontal septum

The horizontal septum (Figure 4d) is extremely thin and reduced; it does not reach to the skin. It lies in the horizontal midline of a myomere up to the point where it is interrupted by the passage of the *n. lateralis* in the myoseptum. There is no horizontal septum in the caudal region.

3.1.4 | Red musculature

The red musculature lies medial to the skin (1) at the posterior border of each myoseptum overlying the white musculature (as exemplified

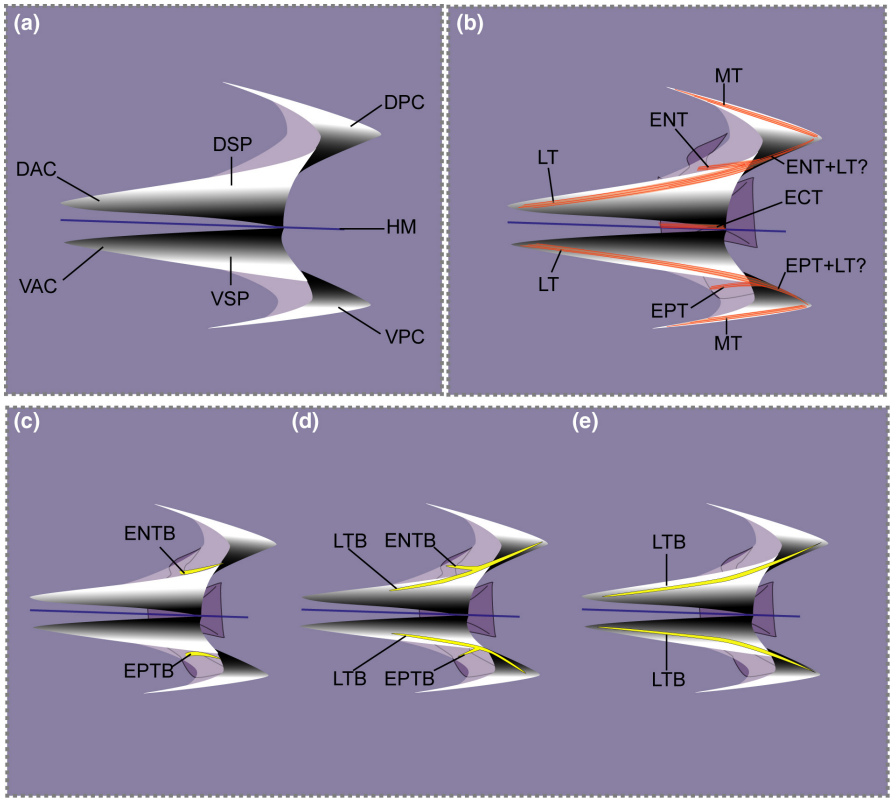

FIGURE 1 Schematic representation of typical myoseptum from midbody in lateral view (anterior to the left). (a) Position of cones in epaxial part (DAC, DPC) and hypaxial part (VAC, VPC) are shown. (b) Arrangement of possible tendons of a myoseptum is shown: epineural tendon (ENT), epipleural tendon (EPT), lateral tendon (LT), epicentral (ECT) and myorhabdoid tendon (MT). It appears as if the fibre bundles of the epineural and lateral tendons merge posteriorly (ENT+LT?/EPT+LT?). (c–e) Three possible ossification patterns resulting in an epineural bone/epipleural bone. (c) Ossification in the epineural tendon (ENTB)/epipelural tendon (EPTB) usually attaching to the neural arch/parapophysis, respectively. (d) Proximally forked epineural/epipleural bone representing ossifications in the epineural tendon/epipleural tendon (ENTB/EPTB) and the lateral tendon (LTB). (e) In myosepta further posteriorly the simple epineural/epipleural bone can be represented by an ossification in the lateral tendon only (LTB). Colour code: orange lines indicate tendons; yellow, ossified intermuscular bone; blue, horizontal midline

in Figure 5c–f) and (2) as two muscle bundles dorsal and ventral to the horizontal midline (exemplified in Figure 5b for *S. affinis*). The red muscle 'packages' at the posterior border of each myomere and dorsal and ventral to the horizontal midline together form a chevron and cover the white musculature laterally. In the anterior body region, 'the chevrons' are narrow (Figure 5b), but they are greatly enlarged and cover the entire white musculature in the posterior body region laterally (see Figure 5 examples for other stomiiform species). The two separate red muscle bundles, directly dorsal and ventral to the horizontal midline, lie medial to this superficial chevron-like red musculature. Within each bundle is a tendon that connects to the myoseptum (Figures 2 and 3; RMTs).

3.1.5 | Caudal tendons

Seven dorsal and seven ventral LTs insert on caudal-fin rays (Figure 2d). The two innermost tendons, inserting on the caudal-fin rays closest to the diastema, are posterior elongations of the LTs of V50 and V51. Those myosepta are the last with an LTB and posterior cones. The LTs, originating in the anterior cones of the following myosepta (V52–V56), extend into the caudal fin and insert on the caudal-fin rays, of which the LT of V56 attaches in the dorsalmost position. Two well-distinguishable MTs insert on the dorsal most/ventral most caudal-fin rays, respectively. There may have been more, weaker posterior MTs that we were not able to visualize, because the last five myosepta have no posterior cones and the medial parts of these myosepta are thin and weakly developed and as a consequence the attachment site of their MTs cannot be determined reliably. The two epaxial and two hypaxial MTs that are still well-distinguishable are most likely those of V52–V53.

3.2 | *Chauliodus sloani* (USNM 200984, MNHN 2021-0225)

3.2.1 | Myosepta

The myosepta show a honeycomb structure (HCS, similar to what is shown in Figure 9a,b for *Eustomias obscurus*) and span 4–4.5 centra

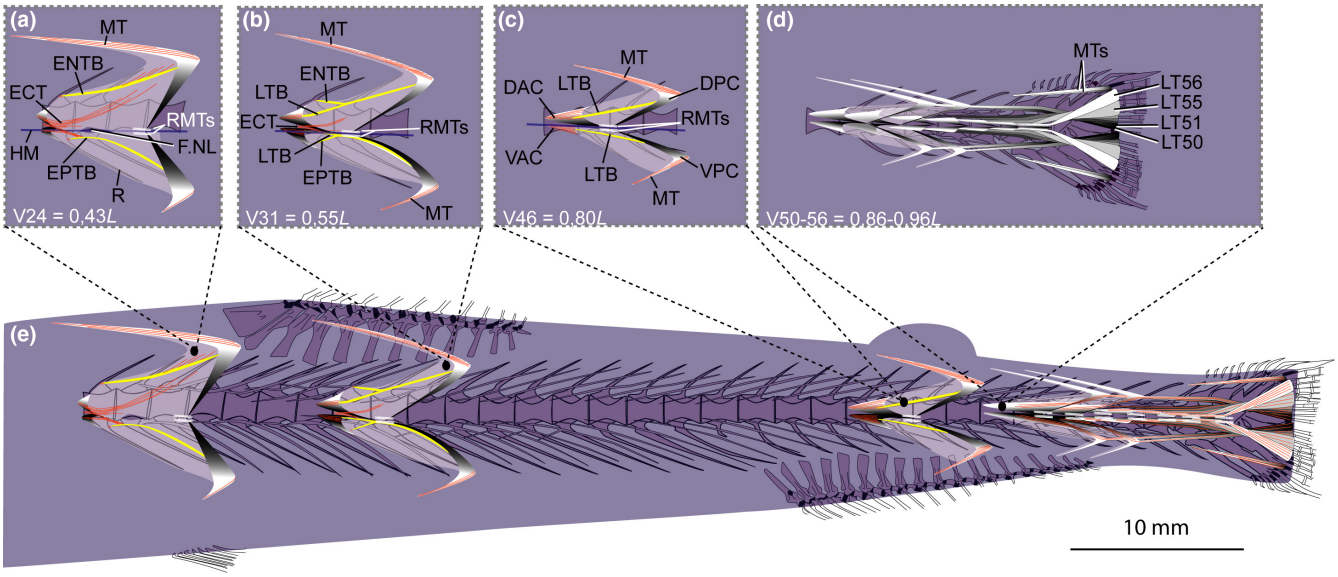

FIGURE 2 Schematic drawing of the musculotendinous system (MTS) of different body regions in *Astronesthes* sp. (MNHN 2000 0576, 118 mm SL). (a) Myoseptum of V24 at 0,43*L*. ENTB and EPTB present. ECT present. (b) Myoseptum of V31 at 0,55*L*. The ENB and EPB are proximally forked. The antero-medial branch (ENTB/EPTB) of the forked intermuscular is attached to the neural arch epaxially and the parapophysis hypaxially, whereas the antero-lateral branch of the forked bony element represents an ossification in the lateral tendon and extends from the DAC/VAC to the DPC/VPC. ECT present. (c) Myoseptum of V46 at 0,80*L*. Intermuscular ossification represents the lateral tendon bone (LTB) epaxially and hypaxially extending from the anterior cones (DAC/VAC) into the posterior cones (DPC/VPC). (d) Caudal tendons that insert on caudal-fin rays and represent LTs of V50–V56. (e) Overview of the different body regions and their MTS. Abbreviations: DAC, dorsal anterior cone; DPC, dorsal posterior cone; ECT, epicentral tendon; ENTB, epineural tendon bone; EPTB, epipleural tendon bone; F.NL, foramen for the *nervus lateralis*; HM, horizontal midline; LT, lateral tendon; LTB, lateral tendon bone; MT, myorhabdoid tendon; R, rib; RMTs, tendons within red muscle bundles; VAC, ventral anterior cone; VPC, ventral posterior cone

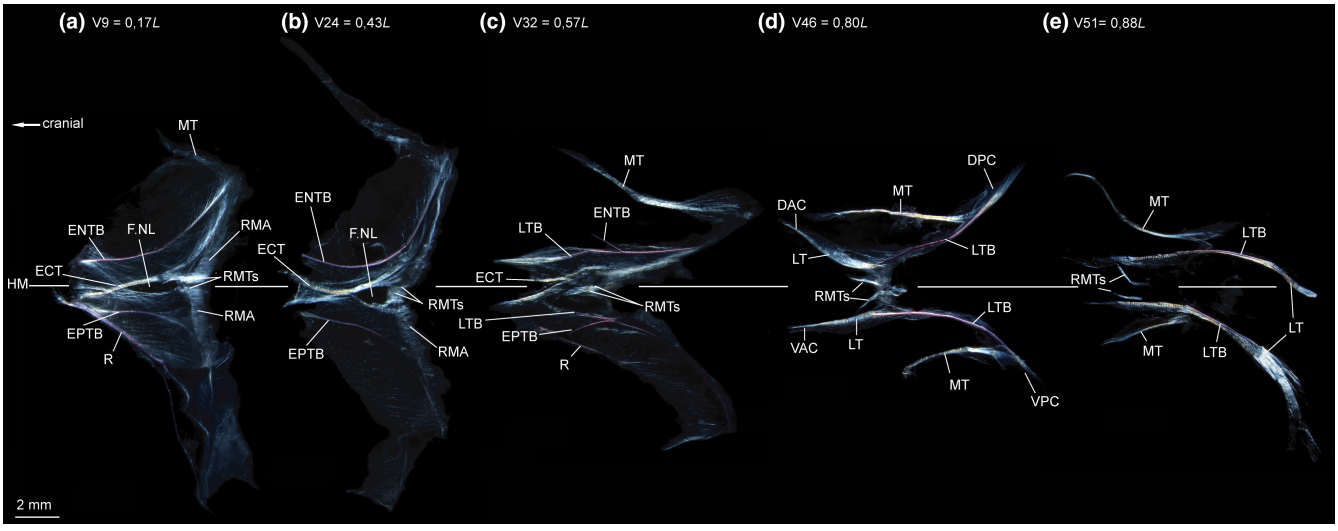

FIGURE 3 Dissected myosepta of *Astronesthes* sp. (MNHN 2000 0576, 118 mm SL) photographed under polarized light. (a) Myoseptum of V9 at 0,17L. ENTB and EPTB present. ECT present, forked distally. Dense connective tissue at posterior border of myoseptum, where red musculature attaches (RMA). RMTs present. (b) Myoseptum of V24 at 0,43*L*. (c) Myoseptum of V32 at 0,57*L*. Anterior cones present; proximally forked intermusculars with ENTB/EPTB as anteromedial branch and LTB as anterolateral branch. (d) Myoseptum of V46 at 0,80*L*. Simple intermuscular ossification represents LTB epaxially and hypaxially extending from anterior (DAC/VAC) into posterior cones (DPC/VPC). (e) Myoseptum of V51 at 0,88*L*. LTs posteriorly elongated to insert on caudal-fin rays. Abbreviations: DAC, dorsal anterior cone; DPC, dorsal posterior cone; ECT, epicentral tendon; ENTB, epineural tendon bone; ENTB, epipleural tendon bone; F.NL, foramen for the *nervus lateralis*; HM, horizontal midline; LT, lateral tendon; LTB, lateral tendon bone; MT, myorhabdoid tendon; R, rib; RMA, attachment site of red musculature; RMTs, tendons within red muscle bundles; VAC, ventral anterior cone; VPC, ventral posterior cone

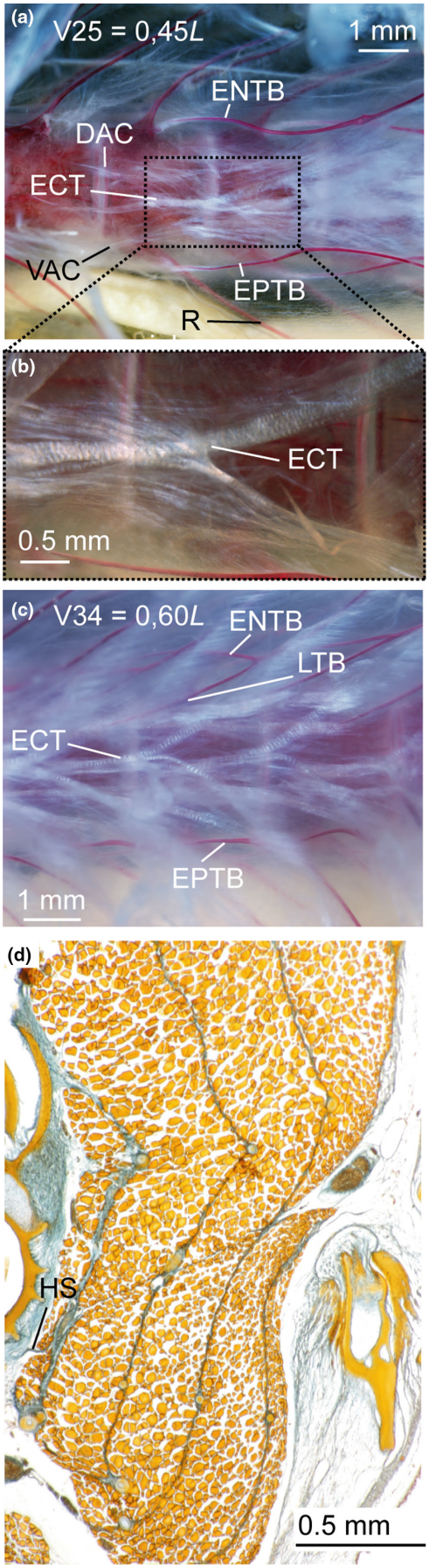

FIGURE 4 Cleared and double-stained specimen of *Astronesthes* sp. (MNHN 2000 0576, 118 mm SL) under polarized light (a–c); and histological serial section of *Astronesthes niger* (MCZ 133101, 62 mm SL). (a) Myoseptum of V25 at 0,45*L*. ENTB, EPTB and ECT present; (b) zoom on distally forked ECT. (c) Myoseptum of V34 at 0,60*L*. Distally forked ECT; proximally forked intermuscular with ENTB/EPTB as anteromedial branch and LTB as anterolateral branch. (d) Transverse serial section showing thin horizontal septum. Abbreviations: DAC, dorsal anterior cone; ECT, epicentral tendon; ENTB, epineural tendon bone; EPTB, epipleural tendon bone; HS, horizontal septum; LTB, lateral tendon bone; R, rib; VAC, ventral anterior cone

until V20 (Figure 6a,e). They become sequentially elongated so that at V27 they span about 5.5 centra (Figure 6b,e). Further posteriorly they become gradually shorter again spanning about 4–4.5 centra at V34 and only 3.5 centra at V48 (Figure 6c,e). The anteriormost myosepta V1–V13 do not have a DAC/VAC (Figure 6a,e); a VAC is present starting at myoseptum V14 and a DAC starting at myoseptum V17. At V47, the DAC spans 1.5 centra in an anterior direction (Figure 6c,e).

3.2.2 | Intermuscular tendons and bones

ECT—In the myosepta of V11–V34, an ECT is present (Figures 6a and 7a,b). Epicentral fibres may be present in preceding myosepta, but could not be identified reliably in our specimens. The ECT inserts in the midline of the centrum and runs along the dorsal and ventral margin of the foramen for the *n. lateralis* (Figures 6a and 7a,b).

ENB/EPB—In the myosepta of V2–V41, an ENTB attaches to the neural arch and extends into the DPC (Figures 6a,b and 7a–d). Posterior to V41, the ENTB is absent, but still present as a tendinous structure (ENT) until V49 (Figure 7e).

In the hypaxial part, the epipleural bone is represented by an ossification in the lateral tendon (LTB) in the myosepta of V2–V46 (Figures 6a–c and 7a–d). In the myosepta of V2–V13, the anterior part of LTB curves dorsally, almost reaching ENTB in the epaxial part (Figures 6a and 7a). With the presence of a VAC, the LTB changes its course and now extends from the VAC into the VPC. In different specimens, forking of the bone is present at different body regions. In specimen USNM 200984 (145 mm SL), the epipleural bone becomes proximally forked between V11 and V16 and in V28. Further posteriorly, the EPT is unossified and present in myosepta up to V49 (Figure 7e).

MT—The MT is present dorsally in all myosepta. Ventrally the MT is developed as a fine tendon starting at V28 (Figure 6e). Starting at V47, ventral secondary anterior cones (VSAC) occur in a couple of myosepta, formed by the ventral MT that turns posteriad (Figures 6c and 7e).

3.2.3 | Horizontal septum

Same as for *Astronesthes*.

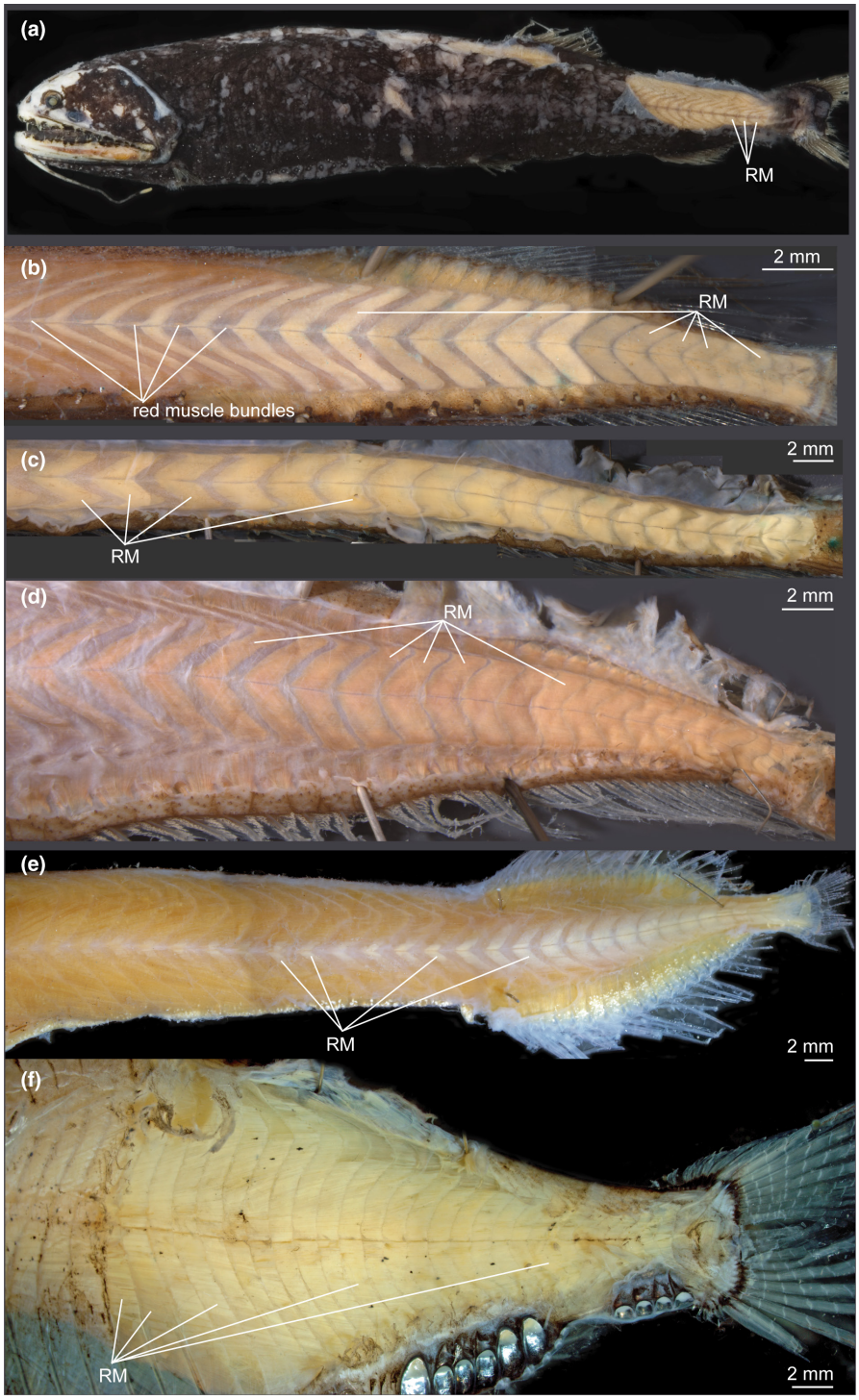

FIGURE 5 Red musculature in ethanol-preserved specimens. Skinned specimens showing superficial red musculature that covers white musculature. Muscle packages are narrow in anterior body region and gradually become larger thus covering entire white musculature in caudal region. Pair of muscle bundles dorsal and ventral the horizontal midline lie medial to superficial red musculature (RM). (a) *Borostomias elucens* (USNM uncat., ca. 110 mm SL). (b) *Stomias affinis* (USNM 358765, 114 mm SL). (c) *Idiacanthus atlanticus* (USNM 206705, 327 mm SL). (d) *Eustomias schmidti* (USNM 261301, 185 mm SL). (e) *Malacosteus niger* (SIO 73-25, 135 mm TL). (f) *Argyropelecus olfersii* (MNHN 2021-0223, 62 mm SL) superficial red musculature covers entire white musculature in all body parts

3.2.4 | Red musculature

Same as for *Astronesthes* except for the following: the RMTs are longer than in *Astronesthes* (Figures 6 and 7; RMTs).

3.2.5 | Caudal tendons

Three dorsal and three ventral LTs insert on caudal-fin rays (Figure 6d,e). The two innermost tendons inserting on the caudal-fin rays closest to

the diastema are posterior elongations of the LTs of V54–V55. The posterior elongated LT of V56 inserts dorsal to the two innermost tendons. There are two dorsal and two ventral MTs that attach to the dorsalmost/ventralmost caudal-fin rays, respectively.

3.3 | *Eustomias simplex* (USNM 372020), *E. obscurus* (USNM 206711)

3.3.1 | Myosepta (*E. simplex*, USNM 372020)

The myosepta span two centra at V45, three centra at V49 and five centra at V54 (Figure 8e). The myosepta and the medial side of the skin show a HCS (Figure 9a–c). Myosepta anterior to the dorsal-fin base (V9–V44) have no well-defined anterior cones (DAC/VAC; Figure 8a,e) and attach to the anterior margin of each centrum. The posterior cones (DPC/VPC) span one successive centrum (Figure 8e). Starting on V45, the myosepta have anterior cones (Figure 8b). Myosepta increase in length sequentially towards the caudal fin through the extreme elongation of the DAC, whereas the DPC becomes shorter (Figure 8e). At their maximum length at V56, the DAC+VAC equal the length of three and a half centra (Figure 8c,e).

3.3.2 | Intermuscular tendons and bones (*E. simplex*, USNM 372020)

ECT—There are no ECTs or ECBs

ENB/EPB—In the myosepta of V1–V50, an ENTB is present, projecting into the DPC (Figures 8a,b and 10a–c). Ventrally, an EPTB is present up to V49 (Figure 10b,c). Both of these intermusculars are simple rod-like ossifications and show no forking. The LT runs parallel to the horizontal septum (Figures 8c and 10c). Due to the dense connective tissue in the area where the red musculature attaches (RMA) to the myoseptum, it is not clear if the LT also runs into the DPC/VPC. In some myosepta between V17 and V43, we found an interrupted LT that runs into the DPC. Caudally, the LTs elongate together with the anterior elongation of DAC/VAC and are continuous tendons stretching from the DAC/VAC to the DPC/VPC (Figures 8e and 10e).

MT—The dorsal and ventral MTs are present up to V60. Ventrally, they are developed at about mid-body.

3.3.3 | Horizontal septum (*E. simplex*, USNM 372020; *E. obscurus*, USNM 206711; *Eustomias filifer*, BMNH 2007.10.31.64)

Same as for *Astronesthes*.

3.3.4 | Red musculature

Same as for *Astronesthes*, but with the following figure reference (Figures 8, 9a–d and 10; RMTs). In the caudal region, the two red muscle bundles occupy the space between the superficial red musculature and the vertebral column (Figure 11c–e).

3.3.5 | Caudal tendons (*E. simplex*, USNM 372020; *E. obscurus*, USNM 206711)

Four dorsal and four ventral LTs insert on caudal-fin rays (Figures 8d,e and 9e). The innermost LTs inserting on caudal-fin rays closest to the diastema originate from myosepta of V60–V61. The epaxial and hypaxial LTs inserting further dorsally/ventrally respectively on caudal-fin rays originate from the myoseptum of V62. The LTs of the compound ural centrum are in continuation at the horizontal midline and insert further dorsally/ventrally on caudal-fin rays. There are two MTs that insert on the dorsalmost and ventralmost caudal-fin rays.

3.4 | *Malacosteus australis* (USNM 296675)

3.4.1 | Myosepta

The myosepta span 2.5 centra at V29 (Figure 12a), two centra at V33, 1.5 centra at V35, almost three centra at V38 (Figure 12b) and 3.5 centra at V41 (Figure 12d). The anteriormost myosepta (V1–V34) have no anterior cone and they insert on the anterior margin of each centrum (Figure 12a,d). At V29, the DPC+VPC reach 1.5 centra in length posteriorly (Figure 12a). The DPC+VPC shorten further caudally, now having the length of one centrum (V33) and only three quarters of a centrum starting at V35 (Figure 12d). A tendinous extension at the tip of the posterior cone reaches the posterior border of the following centrum (Figure 12b,d).

At V35, the DAC becomes anteriorly elongated and spans two anterior centra at its maximum length (e.g., V41; Figure 12d). The myosepta anterior to V33 have a secondary anterior cone (VSAC) in the hypaxial part of the myoseptum (Figures 12a,d and 13b).

3.4.2 | Intermuscular tendons and bones

ECT—On V1–V32, there is an ECT attaching to the midline of the centrum. It bifurcates distally and forms a canal in the myoseptum for passage of the *n. lateralis* (Figures 12a,d and 13b).

ENB/EPB—Up to V32, all myosepta possess an ENTB. An EPTB is present up to V33 (Figures 12d and 13a,b). Each ENTB attaches to its respective neural arch and the EPTB to its respective parapophysis. There are no LTs in the myosepta of V1–V34. Starting on V35, the LTs are present, but interrupted, and do not extend continuously from the anterior to the posterior cones. There are dorsal and ventral LTs present, which run parallel to the horizontal septum (Figures 12b,d and 13c,d), and only single fibre tracts turn dorsally/ventrally and disappear quite soon in the course of the ESP/HSP. The posterior part of the LT

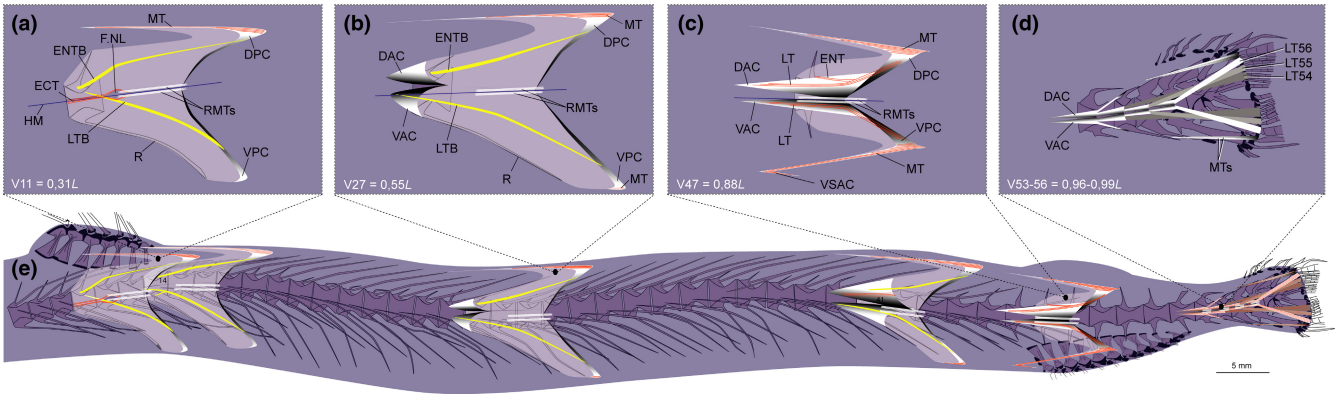

FIGURE 6 Schematic drawing of musculotendinous system (MTS) of different body regions in *Chauliodus sloani* (USNM 200984, 145 mm SL). (a) Myoseptum of V11 at 0,31*L*. ENTB present. In hypaxial part of the myoseptum, the ossification represents an LTB, pointing to neural arch. ECT present. (b) Myoseptum of V27 at 0,55*L*. Anterior cones present. Ventral LTB projects into VAC. (c) Myoseptum of V47 at 0,88*L*. Simple intermuscular ossification represents LTB epaxially and hypaxially extending from anterior (DAC/VAC) into posterior cones (DPC/VPC), respectively. Dorsally there is an ENT present. Ventrally, the MT turns posteriad and forms a VSAC. (d) Caudal tendons that insert on caudal-fin rays and represent LTs of V54–V56. (e) Overview of different body regions and their MTS. Abbreviations: DAC, dorsal anterior cone; DPC, dorsal posterior cone; ECT, epicentral tendon; ENT, epineural tendon; ENTB, epineural tendon bone; F.NL, foramen for the *nervus lateralis*; HM, horizontal midline; LT, lateral tendon; LTB, lateral tendon bone; MT, myorhabdoid tendon; R, rib; RMTs, tendons within red muscle bundles; VAC, ventral anterior cone; VPC, ventral posterior cone; VSAC, ventral secondary anterior cone

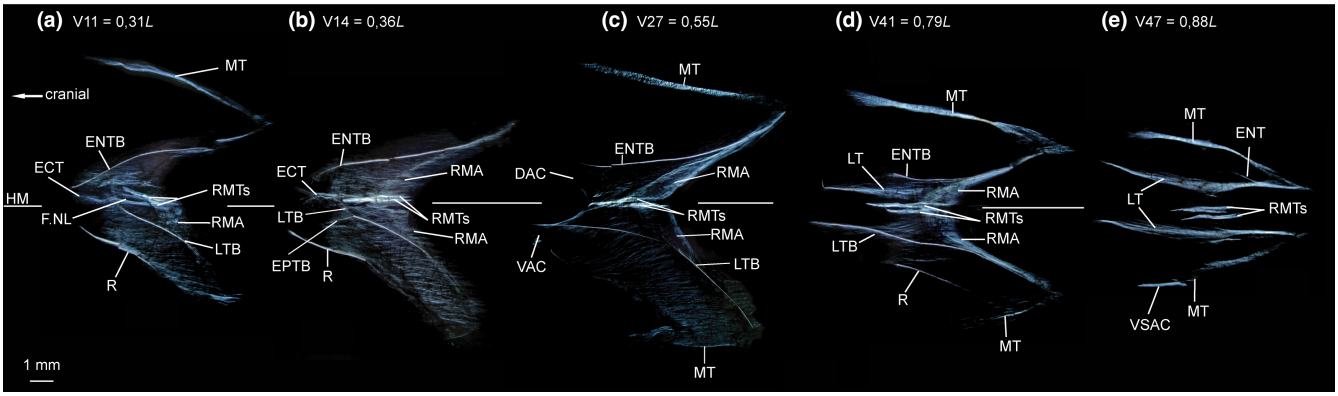

FIGURE 7 Dissected myosepta of *Chauliodus sloani* (USNM 200984, 145 mm SL) photographed under polarized light. (a) Myoseptum of V11 at 0,31*L*. Simple epineural (ENTB) present. In hypaxial part of the myoseptum, the ossification represents an LTB, pointing to neural arch. Epicentral (ECT) present. (b) Myoseptum of V14 at 0,36*L*. Simple epineural (ENTB) present. The intermuscular in ventral part of myoseptum is proximally forked, with an EPTB as anteromedial branch and an LTB as anterolateral branch. (c) Myoseptum of V27 at 0,55*L*. Anterior cones present. Ventral LTB projects into VAC. (d) Myoseptum of V41 at 0,79*L*. Simple intermuscular ossification represents LTB epaxially and hypaxially extending from anterior (DAC/VAC) into posterior cones (DPC/VPC). Dorsally there is an epineural tendon (ENT) present. Ventrally, the MT turns posteriad and forms a ventral secondary anterior cone (VSAC). (e) Myoseptum of V47 at 0,88*L* Abbreviations: DAC, dorsal anterior cone; DPC, dorsal posterior cone; ECT, epicentral tendon; ENT, epineural tendon; ENTB, epineural tendon bone; EPTB epipleural tendon bone; F.NL, foramen for the *nervus lateralis*; HM, horizontal midline; LT, lateral tendon; LTB, lateral tendon bone; MT, myorhabdoid tendon; R, rib; RMA, attachment site of red musculature; RMTs, tendons within red muscle bundles; VAC, ventral anterior cone; VPC, ventral posterior cone; VSAC, ventral secondary anterior cone

is present in the DPC/VPC (Figures 12b,d and 13c,d). Starting with the myoseptum associated with V41, the LTs are continuous tendons extending from the DAC/VAC to the DPC/VPC (Figures 12d and 13e).

MT—Epaxial MTs are present in all investigated myosepta. Hypaxial MTs are present in myosepta posterior to V15. In myosepta of V16–V33, there is a VSAC, formed by the ventral MT that turns posteriad (Figures 12a,d and 13b).

3.4.3 | Horizontal septum

Same as for *Astronesthes*.

3.4.4 | Red musculature

Same as for *Astronesthes* (Figures 5e, 12, and 13; RMTs).

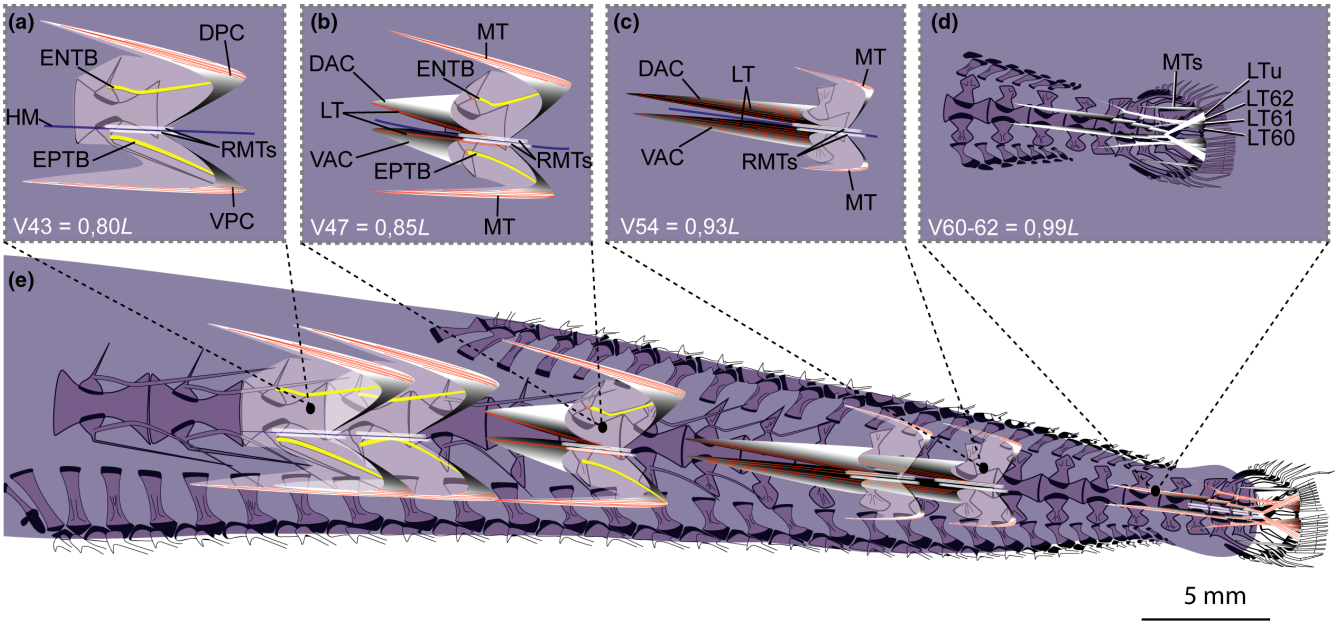

FIGURE 8 Schematic drawing of musculotendinous system (MTS) of different body regions in *Eustomias simplex* (USNM 372020, 223 mm SL). (a) Myoseptum of V43 at 0,80*L*. ENTB and EPTB present. (b) Myoseptum of V47 at 0,85*L*. Anterior cones present. LTs run parallel to HM. (c) Myoseptum of V54 at 0,93*L*. Dorsal elongation of DAC/VAC. (d) Caudal tendons that insert on caudal-fin rays and represent LTs of V60–V62 + LT of compound ural centrum. (e) Overview of different body regions and their MTS. Abbreviations: DAC, dorsal anterior cone; DPC, dorsal posterior cone; ENTB, epineural tendon bone; EPTB epipleural tendon bone; HM, horizontal midline; LT, lateral tendon; LTu, lateral tendon of compound ural centrum; MT, myorhabdoid tendon; RMTs, tendons within red muscle bundles; VAC, ventral anterior cone; VPC, ventral posterior cone

3.4.5 | Caudal tendons

Four dorsal and four ventral tendons insert on caudal-fin rays (Figure 12c,d). They originate from the myosepta of V45–V47 (LT45–47) and the myoseptum that is associated with the compound ural centrum (LTu). The two innermost tendons inserting on caudal-fin rays closest to the diastema are posterior elongations of the dorsal and ventral LTs of V45. The LTs of V46 and V47 insert dorsal/ventral to those two innermost tendons. The dorsal and ventral LTs of the compound ural centrum insert further dorsally/ventrally on caudal-fin rays. The MTs of myoseptum 47 insert on the dorsalmost/ventralmost caudal-fin rays.

3.5 | *Sigmops elongatus* (MNHN 2003 1394)

3.5.1 | Myosepta

The anteriormost myosepta, those anterior to V18 span about 3–3.5 centra (Figure 14a,d). They lengthen sequentially and span about 5 centra at V31 (Figure 14b,d). Myosepta anterior to the dorsal- and anal-fin bases (V1–V18) have no well-defined anterior cones (DAC/VAC; Figure 14a,d) and attach to the anterior margin of each centrum. The posterior cones extend two centra posteriorly (Figure 14a,d). Starting on V21, the myosepta have anterior cones (Figure 14b,d). The myosepta increase in length towards the caudal fin through anterior elongation of the DAC/VAC, as well as posterior elongation of the DPC/VPC. At their maximum length (V31), the anterior cones span one preceding centrum, whereas the posterior cones span three posterior centra (Figure 14d).

3.5.2 | Intermuscular tendons and bones

ECT—In the myosepta of V1–V17, a single ECT is present (Figure 15a). It inserts on the midline of the centrum, runs along the dorsal margin of the foramen for the *n. lateralis* and further into the DPC (Figures 14a and 15a). From V18 on, the ECT shortens, and is present as a double structure dorsal and ventral to the HM (Figures 14b and 15b). There is no ECT posterior to V27 (Figure 15c).

ENB/EPB—In the myosepta of V1–V21, an ENTB attaches to the neural arch (Figures 14a and 15a). In front of the first neural arch and within the third occipital myoseptum an accessory neural arch (see Britz & Johnson, 2010; Johnson & Britz, 2010, for clarification of the term and its occurrence among teleosts) and a free ENTB are present. ENTs are unossified in the myosepta of V22–V27 (Figures 14b and 15b). Further posteriorly, there are no ENBs or ENTs (Figure 15c).

In the myosepta of V15–V25, an EPTB attaches to the parapophysis (Figures 14a and 15a). The posterior most EPTBs are shorter than the anterior ones (Figure 14d). EPTs are unossified in the myosepta of V26–V28 (Figure 14d). Further posterior, there are no EPBs or EPTs (Figures 14d and 15c). All intermuscular bones are unforked. An LT is present in all myosepta with an anterior cone (Figure 14d).

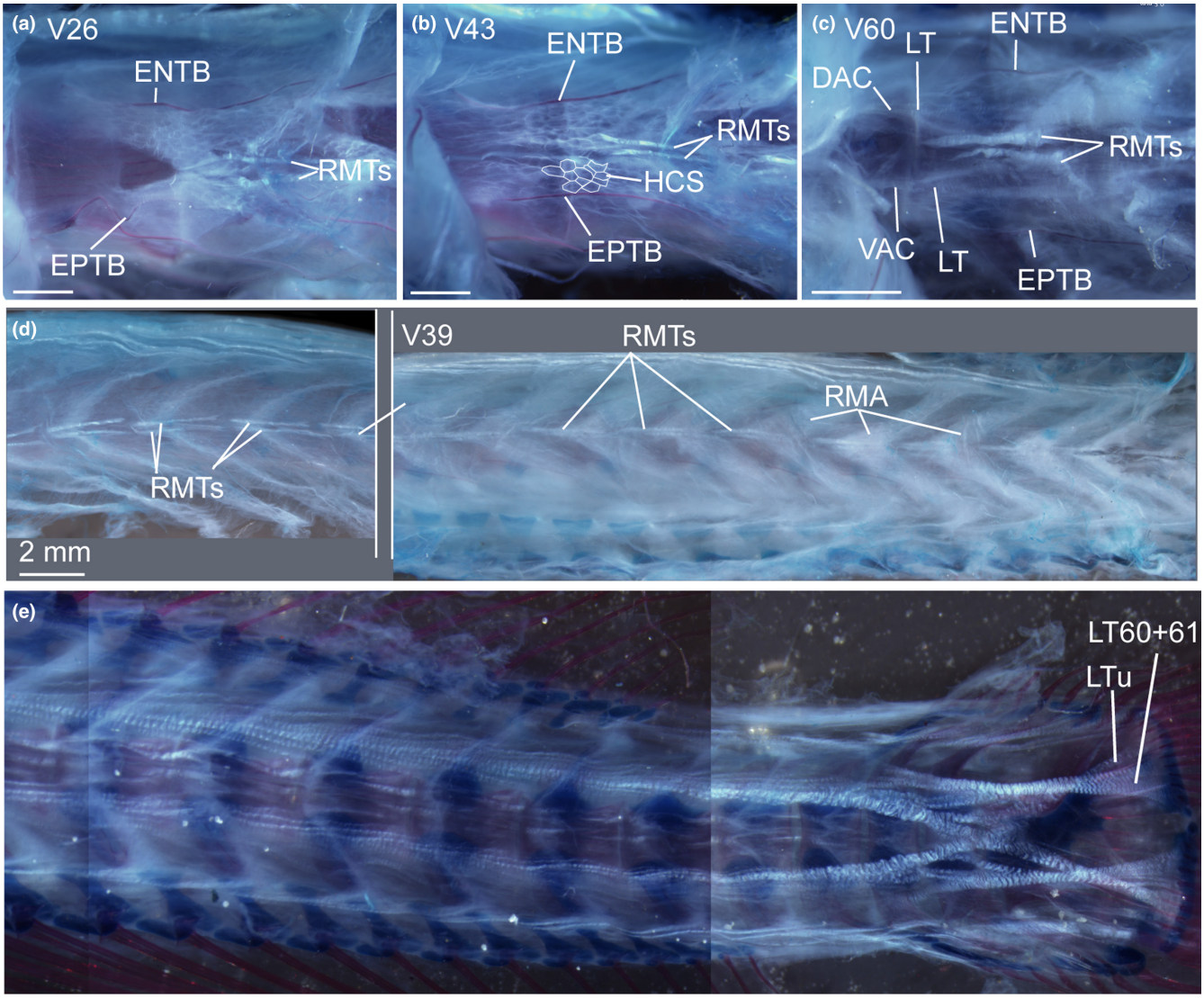

FIGURE 9 Cleared and double stained specimen of *Eustomias obscurus* (USNM 206711, 199 mm SL) under polarized light. (a) Myoseptum of V26. ENTB and EPTB present. Tendons within red musculature (RMTs) that run parallel to HM. (b) Myoseptum of V43. See description in (a) and note honeycomb structure of myoseptum (traced in parts hypaxially for better visualization). (c) Myoseptum of V60. See description in (a). (d) Overview of RMTs and attachment site for red musculature (RMA) in different body regions. (e) Caudal tendons. Abbreviations: DAC, dorsal anterior cone; ENTB, epineural tendon bone; EPTB, epipleural tendon bone; LT, lateral tendon; LTu, lateral tendon of compound ural centrum; RMA, attachment site of red musculature; RMTs, tendons within red muscle bundles; VAC, ventral anterior cone. Scale bars if not otherwise noted: 1 mm

MT—An epaxial MT is present in all myosepta. Hypaxial MTs are present as a fine tendon as of V17. The MTs reach a maximum length in the myoseptum associated with V31 and shorten again posteriorly.

3.5.3 | Horizontal septum

Same as for *Astronesthes*.

3.5.4 | Red musculature

Same as for *Astronesthes*, except for the following: the tendons in the two red muscle bundels, dorsal and ventral to the horizontal midline, are sheet-like and resemble aponeuroses that connect to a myoseptum (Figures 14 and 15; RMTs).

3.5.5 | Caudal tendons

Four dorsal and four ventral tendons insert on caudal-fin rays (Figure 14c,d). They are all LTs, originating from the last four myosepta (LT37–40). The two innermost tendons inserting on caudal-fin rays closest to the diastema are posterior elongations of the LTs of V37. The LTs of V38 and V39 insert dorsal/ventral to those two inner tendons. The LTs of V40 insert further dorsally/ventrally on caudal-fin rays. Two MTs insert on the dorsalmost/ventralmost caudal-fin rays respectively.

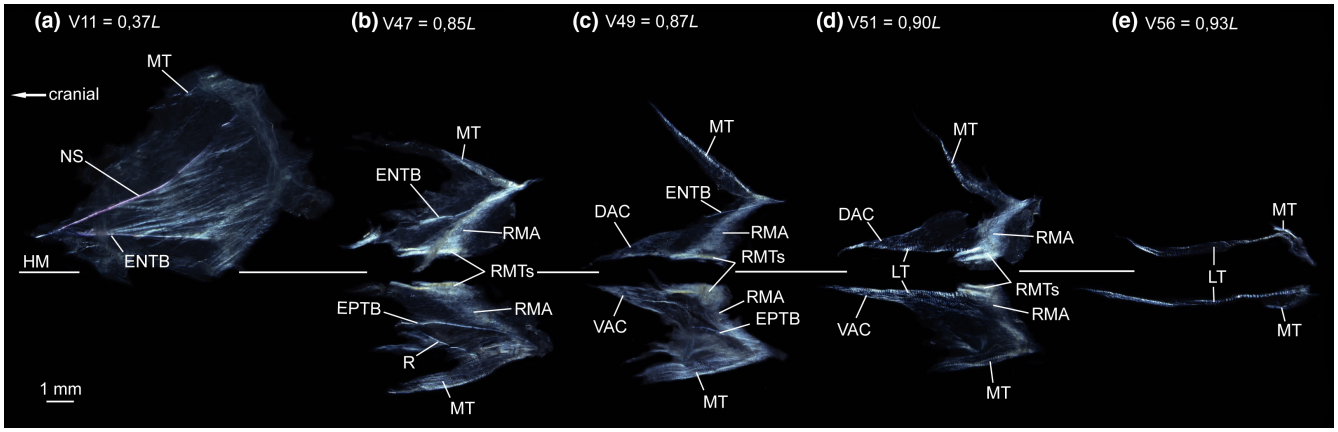

FIGURE 10 Dissected myosepta of *Eustomias simplex* (USNM 372020, 223 mm SL) photographed under polarized light. (a) Dorsal part of myoseptum of V11 at 0,37*L*. ENTB present. (b) Myoseptum of V47 at 0,85*L*. ENTB/EPTB present. (c) Myoseptum of V49 at 0,87*L*. ENTB and EPTB shorten with tendinous attachment further dorsal/ventral on neural spine/haemal spine. (d) Myoseptum of V51 at 0,90*L*. Dorsal and ventral LTs run parallel to HM. (e) Myoseptum of V56 at 0,93*L*. DAC/VAC anteriorly elongated. Dorsal and ventral LTs run parallel to HM. Abbreviations: DAC, dorsal anterior cone; DPC, dorsal posterior cone; ENTB, epineural tendon bone; EPTB epipleural tendon bone; HM, horizontal midline; LT, lateral tendon; MT, myorhabdoid tendon; NS, neural spine; RMA, attachment site of red musculature; RMTs, tendons within red muscle bundles; VAC, ventral anterior cone; VPC, ventral posterior cone

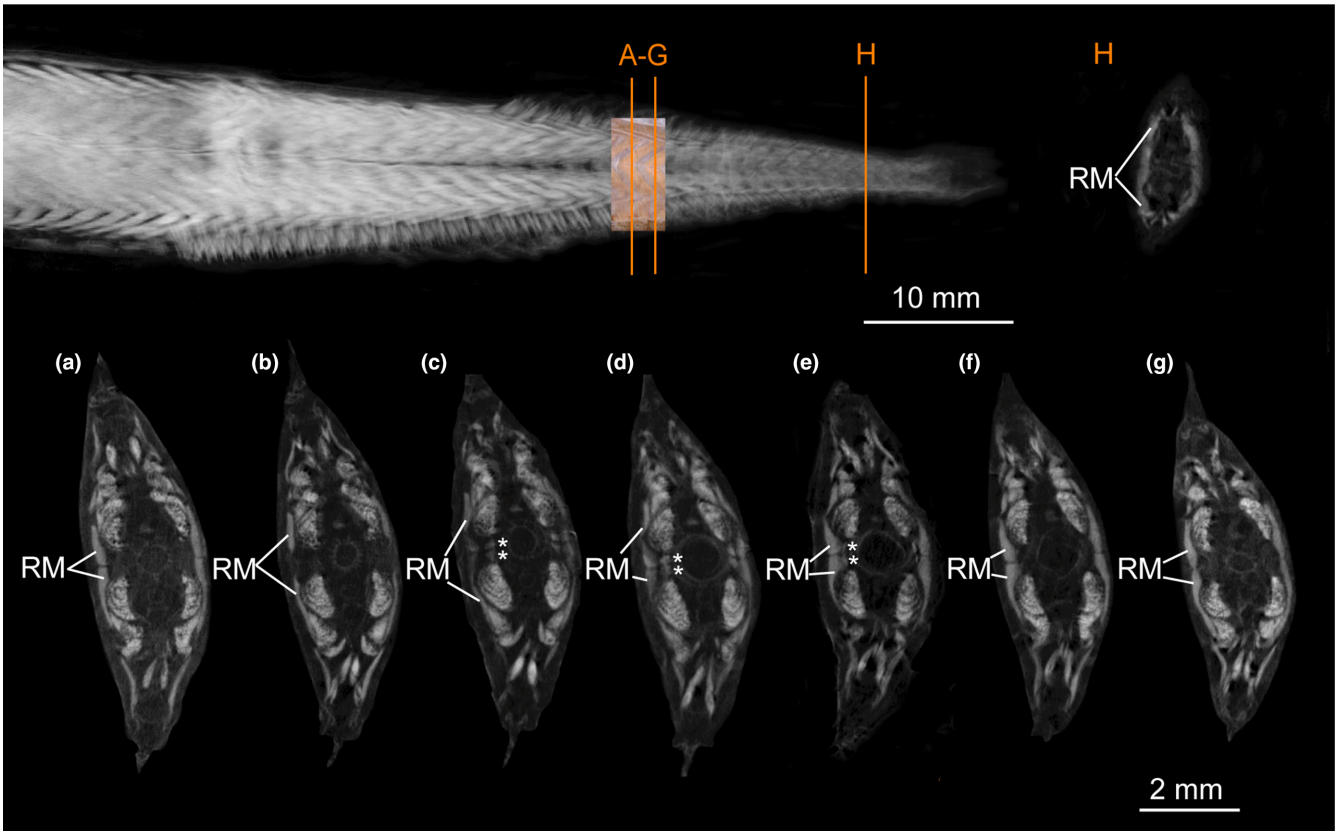

FIGURE 11 Micro-CT scan of *Eustomias schmidti* (USNM 261301, 185 mm SL) stained with iodine to visualize muscles. (a–g) Different sections of red musculature (RM) between middle part of a myomere to middle part of following myomere (orange lines in overview show positions of sections shown in (a) and (g). (a) Section through middle part of superficial RM. (b) Superficial RM spread dorsally and ventrally. (c–e) Paired bundles of RM appear (marked with an *) between superficial RM (of following myomere) and vertebral column and occupy space between widely separate dorsal and ventral anterior cones. (f–g) Middle part of following superficial RM (in these sections the paired bundles are not visible as they are tendinous (RMT). (h) Amount of superficial RM further posterior increased

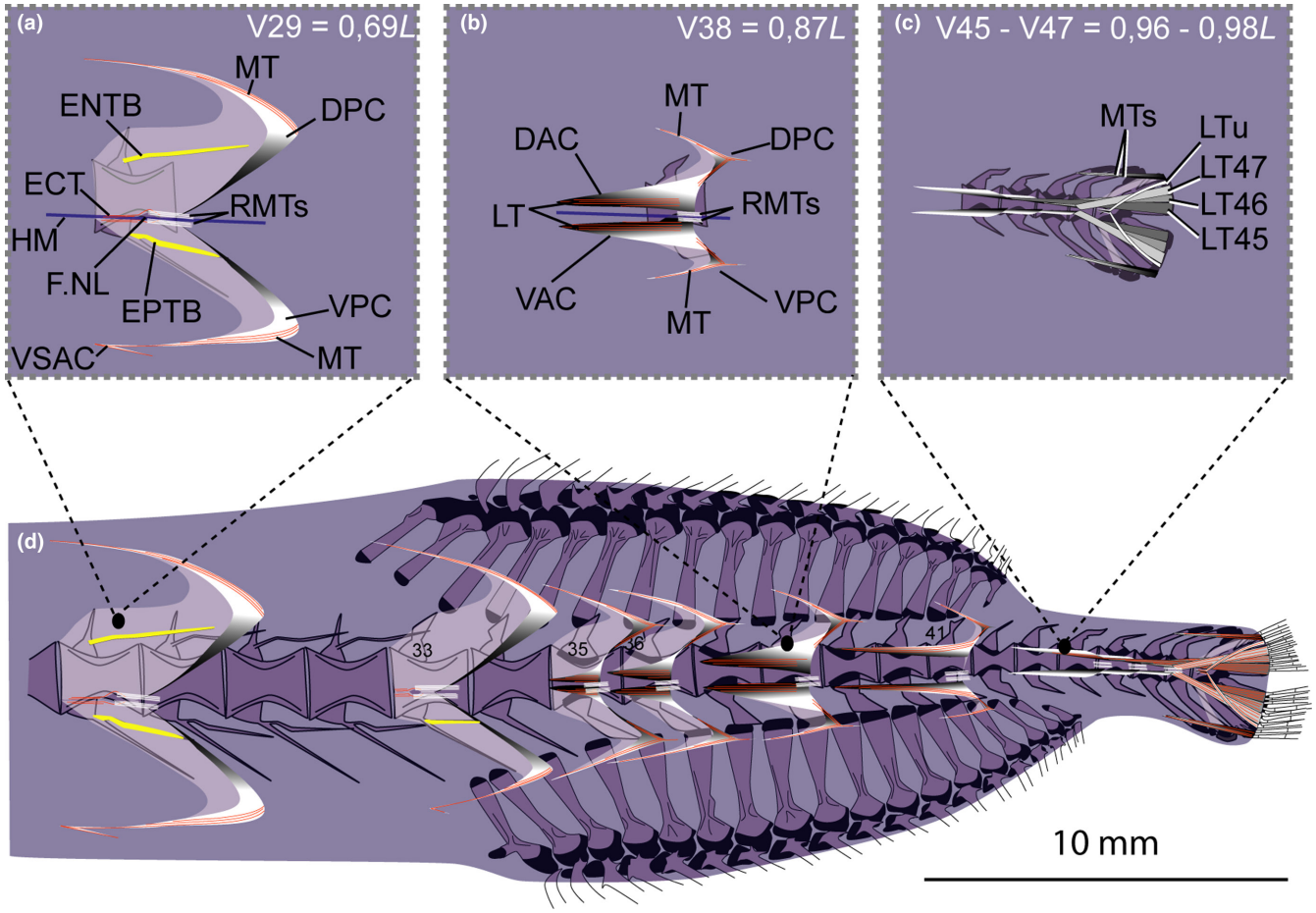

FIGURE 12 Schematic drawing of musculotendinous system (MTS) of different body regions in *Malacosteus australis* (USNM 296675, 110 mm SL). (a) Myoseptum of V29 at 0,69*L*. There is no DAC/VAC. ENTB and EPTB present. VSAC present. (b) Myoseptum of V38 at 0,87*L*. Anterior cones present. LTs run parallel to HM, are interrupted in sloping parts and again present in posterior cones. Tip of posterior cones posteriorly elongated. (c) Tendons that insert on caudal-fin rays and represent LTs of V45-V47 + LT of compound ural centrum. (d) Overview of different body regions and their MTS. Abbreviations: DAC, dorsal anterior cone; DPC, dorsal posterior cone; ENTB, epineural tendon bone; EPTB epipleural tendon bone; F.NL, foramen for the *nervus lateralis*; HM, horizontal midline; LT, lateral tendon; LTu, lateral tendon of compound ural centrum; MT, myorhabdoid tendon; RMTs, tendons within red red muscle bundles; VAC, ventral anterior cone; VSAC, ventral secondary anterior cone; VPC, ventral posterior cone

3.6 | *Polymetme* sp. (MNHN 1997 830)

3.6.1 | Myosepta

The myosepta span about four centra in the body region anterior to the dorsal fin. The anteriormost myosepta (V1–V14) have a small DAC, reaching slightly over the anterior border of its corresponding centrum. There is no well-defined DPC in myosepta of V1–V20 (Figure 16a). The DAC gradually elongates and extends to the anterior border of its preceding centrum at V17 (Figure 16a). In this mid-body region (below the dorsal fin), a myoseptum spans five centra (Figure 16b). The myoseptum reaches its maximum dimension at V30 where it spans 6.5 centra. The anterior cones almost extend to the anterior border of the second preceding centrum, and the posterior cones almost extend to the posterior border of the third successive centrum (Figure 16c,e).

3.6.2 | Intermuscular tendons and bones

ECT—In the myosepta of V1–V25, an ECT is present (Figures 16a,b and 17a–c). In the anteriormost myosepta, it inserts below the midline on the rib, runs along the dorsal margin of the foramen for the *n. lateralis* and further into the DPC (Figures 16a and 17a–c). It inserts dorsally on the parapophysis as of V15. From V20 on, the ECT shortens, no longer extends into the DPC and inserts in the midline of the centrum (Figure 16b).

ENB/EPB—In the myosepta of V1–V24, a simple ENTB attaches to the neural arch (Figures 16a and 17a–c). The last five ENTBs attach further dorsally on the neural spines (Figure 16b). In the myosepta of V25–V31, only tendons (ENT) are present (Figures 16c and 17e). EPTBs are present in the myosepta of V15–V23 (Figures 16a,b and 17b,c). The EPTB is very short in V15 where it attaches to the rib. The following three EPTBs attach to the parapophysis, and the last five attach further ventrally on the haemal spine (Figure 16e). Starting on V31, only LTs are present in the myosepta (Figure 17f).

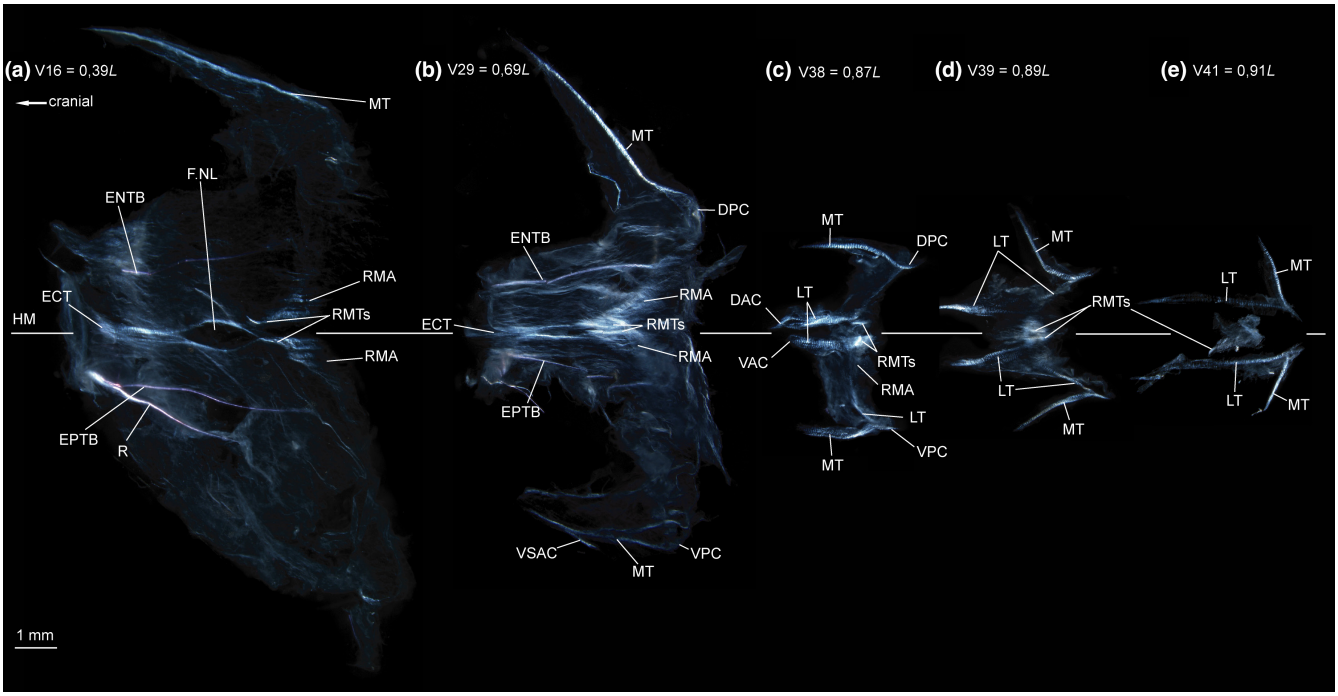

FIGURE 13 Dissected myosepta of *Malacosteus australis* (USNM 296675, 110 mm SL) photographed under polarized light. (a) Myoseptum of V16 at 0,39*L*. ECT, ENTB and EPTB present. Dense connective tissue in insertion area of red musculature (RMA). (b) Myoseptum of V29 at 0,69*L*. ECT, ENTB and EPTB present. VSAC present. Tendons within bundles of RM dorsal and ventral to HM. (c) Myoseptum of V38 at 0,87*L*. LTs present, however, interrupted in sloping parts. (d) Myoseptum of V39 at 0,89*L*. LTs present, however, interrupted in sloping parts. (e) Myoseptum of V41 at 0,91*L*. DAC/VAC anteriorly elongated. LTs continuous from anterior cones to posterior cones. Abbreviations: DAC, dorsal anterior cone; DPC, dorsal posterior cone; ECT, epicentral tendon; ENTB, epineural tendon bone; EPTB, epipleural tendon bone; F.NL, foramen for the *nervus lateralis*; HM, horizontal midline; LT, lateral tendon; MT, myorhabdoid tendon; R, rib; RMA, attachment site of red musculature; RMTs, tendons within red muscle bundles; VAC, ventral anterior cone; VSAC, ventral secondary anterior cone; VPC, ventral posterior cone

MT—The epaxial and hypaxial MTs are present in all investigated myosepta, with the exception that the ventral MT is missing in myosepta anterior to V15. MTs reach their maximum length at V30 (Figures 16 and 17).

3.6.3 | Horizontal septum

Same as for *Astronesthes*.

3.6.4 | Red musculature

Same as for *Astronesthes* except for the following: The two red muscle bundles dorsal and ventral to the horizontal midline have only in the caudal region small tendons that connect to a myoseptum (Figures 16 and 17; RMTs).

3.6.5 | Caudal tendons

Same as for *S. elongatus* except for the following: The caudal tendons in *Polymetme* sp. are LTs of the myosepta of V38–V41 (Figure 16d,e).

3.7 | *Argyropelecus affinis* (MNHN 2021-0224), *Argyropelecus olfersii* (MNHN 2021-0223)

3.7.1 | Myosepta

At V14, the myosepta span about three centra (Figure 18a). Myosepta anterior to the dorsal- and anal-fin bases (V1–V8) have no well-defined anterior cone (DAC/VAC; Figure 19a) and attach to the anterior margin of the respective centrum. At V14, the DAC extends to the anterior border of the preceding centrum, whereas the VAC is shorter and only extends to the middle of the preceding centrum. The DPCs/VPCs extend to the posterior border of the succeeding centrum. The DACs/VACs elongate gradually, and the myosepta span about five centra at V23. The posterior border of the first eight myosepta is tendinous (T; Figure 19a), a condition only found in this species.

We found a peculiarity in our specimen starting at V26. There the DAC/VAC are turned upward/downward, so that the tip of the cones point dorsally/ventrally. In the succeeding myoseptum, associated with V27, the VAC turns posteriad. The DACs/VACs of V28–V31 point all posteriad. They are again directed anteriad on V32. We were not able to check this condition in a second specimen of *Argyropelecus affinis* for lack of material; however, all anterior cones were normal and anteriorly directed in our specimen of *Argyropelecus olfersii*. Interestingly, in one

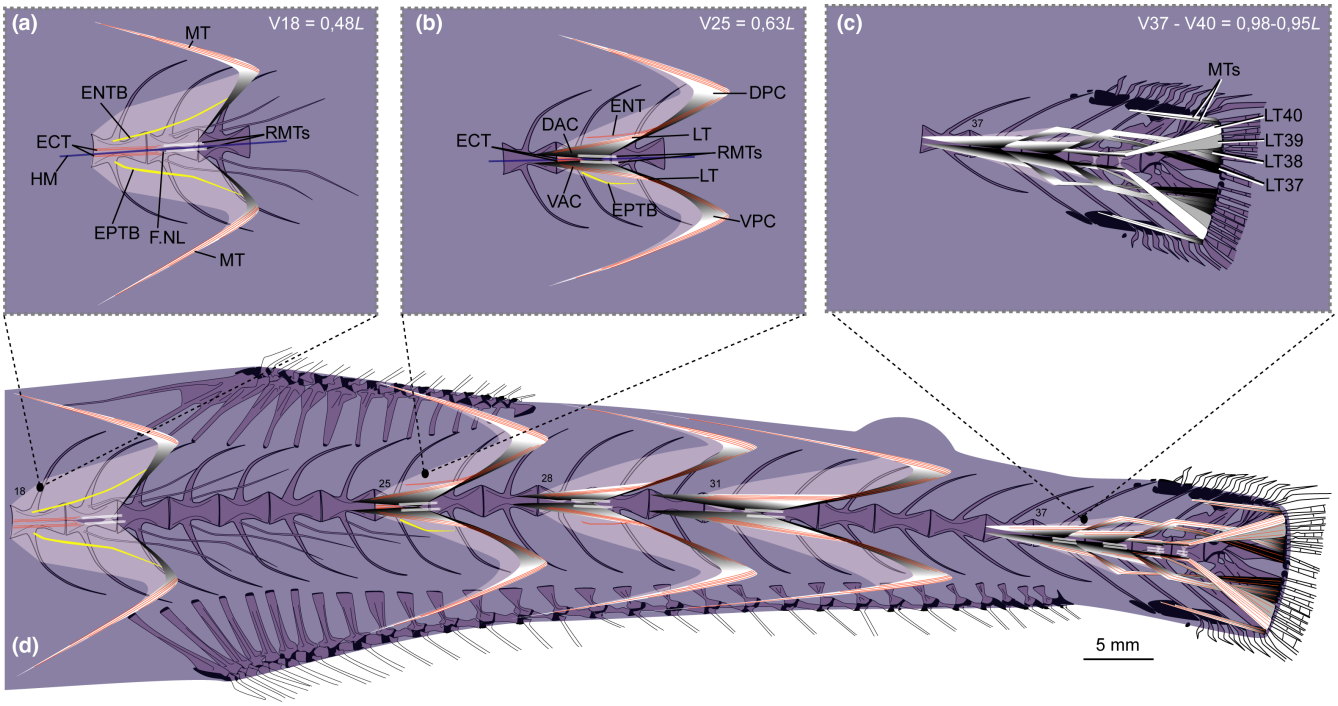

FIGURE 14 Schematic drawing of musculotendinous system (MTS) of different body regions in *Sigmops elongatus* (MNHN 2003 1394, 175 mm SL). (a) Myoseptum of V18 at 0,48*L*. There is no DAC/VAC. ECT, ENTB and EPTB present; (b) Myoseptum of V25 at 0,63*L*. Anterior cones present. LTs extending from anterior to posterior cones. Dorsally there is an ENT and ventrally still an EPTB present. (c) Tendons that insert on caudal-fin rays and represent LTs of V37–V40. (d) Overview of different body regions and their MTS. Abbreviations: DAC, dorsal anterior cone; DPC, dorsal posterior cone; ECT, epicentral tendon; ENT, epineural tendon; ENTB, epineural tendon bone; EPTB, epipleural tendon bone; F.NL, foramen for the *nervus lateralis*; HM, horizontal midline; LT, lateral tendon; MT, myorhabdoid tendon; RMTs, tendons within red muscle bundles; VAC, ventral anterior cone; VPC, ventral posterior cone.

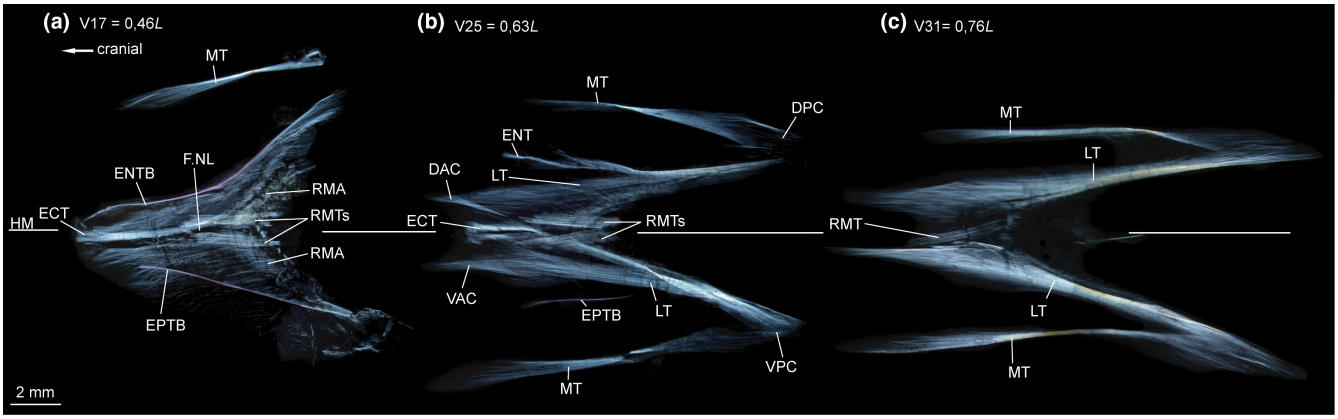

FIGURE 15 Dissected myosepta of *Sigmops elongatus* (MNHN 2003 1394, 175 mm SL) photographed under polarized light. (a) Myoseptum of V17 at 0,46*L*. ECT, ENTB and EPTB present. Dense connective tissue in insertion area of the superficial RM and tendons dorsal and ventral to HM within the bundles of RM. (b) Myoseptum of V25 at 0,63*L*. ECT, ENT and EPTB present. LTs extending from anterior into posterior cones. (c) Myoseptum of V31 at 0,76*L*. LTs present. Abbreviations: DAC, dorsal anterior cone; DPC, dorsal posterior cone; ECT, epicentral tendon; ENTB, epineural tendon bone; EPTB, epipleural tendon bone; F.NL, foramen for the *nervus lateralis*; HM, horizontal midline; LT, lateral tendon; MT, myorhabdoid tendon; RMA, attachment site of red musculature; RMTs, tendons within red muscle bundles; VAC, ventral anterior cone; VPC, ventral posterior cone

specimen of *Vinciguerria lucetia* (SIO 95-123, 45 mm), we found a similar pattern with several anterior cones posteriorly directed. At this point we cannot decide whether such morphological condition represents a malformation or a modification found in some mesopelagic fishes.

3.7.2 | Intermuscular tendons and bones

ECT—There is a small double ECT present up to V20 (Figures 18a and 19a,b).

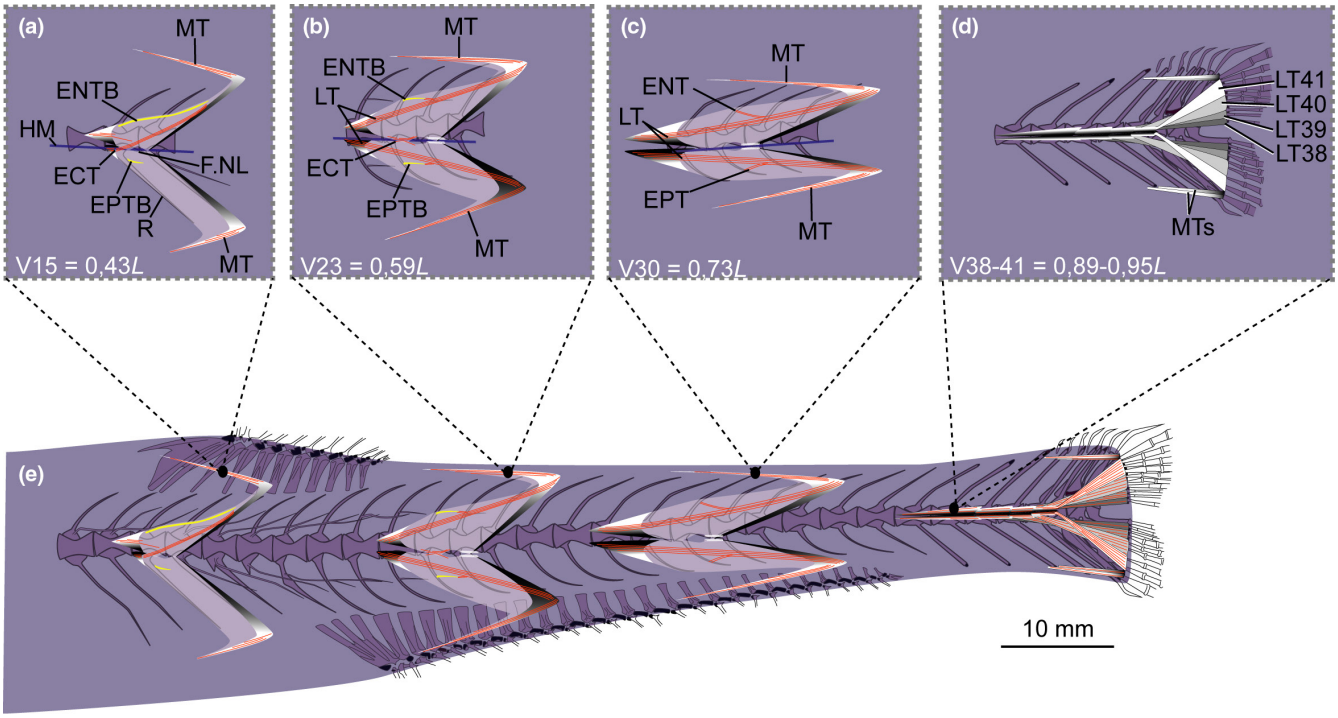

FIGURE 16 Schematic drawing of musculotendinous system (MTS) of different body regions in *Polymetme* sp. (MNHN 1997 830, 160 mm SL). (a) Myoseptum of V15 at 0,43*L*. DAC/VAC present. ECT, ENTB and EPTB present. (b) Myoseptum of V23 at 0,59*L*. LTs extending from anterior into posterior cones. ECT, ENTB and EPTB present. (c) Myoseptum of V30 at 0,73*L*. LTs extending from the anterior into posterior cones. ENT and EPT present. (d) Tendons that insert on caudal-fin rays and represent LTs of V38–V41. (e) Overview of different body regions and their MTS. Abbreviations: DAC, dorsal anterior cone; DPC, dorsal posterior cone; ECT, epicentral tendon; ENT, epineural tendon; ENTB, epineural tendon bone; EPT, epipleural tendon; EPTB, epipleural tendon bone; F.NL, foramen for the *nervus lateralis*; HM, horizontal midline; LT, lateral tendon; MT, myorhabdoid tendon; RMTs, tendons within red muscle bundles; VAC, ventral anterior cone; VPC, ventral posterior cone

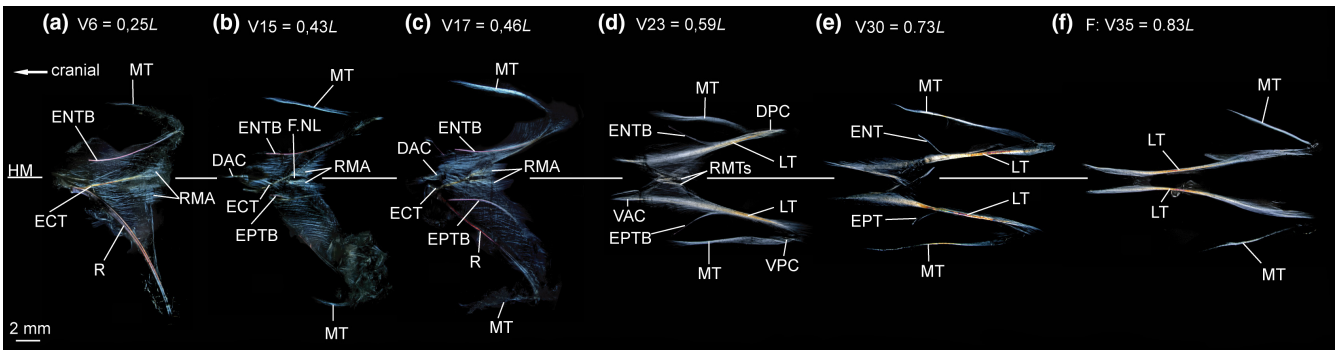

FIGURE 17 Dissected myosepta of *Polymetme* sp. (MNHN 1997 830, 160 mm SL) photographed under polarized light. (a) Myoseptum of V6 at 0,25*L*. ECT and ENTB present. Dense connective tissue in insertion area of RM. (b) Myoseptum of V15 at 0,43*L*. ECT, ENTB and EPTB present. (c) Myoseptum of V17 at 0,46*L*. Anterior cones present. (d) Myoseptum of V23 at 0,59*L*. LTs, ENTB and EPTB present. LTs extending from anterior into posterior cones. (e) Myoseptum of V30 at 0,73*L*. LTs, ENT and EPT present. (f) Myoseptum of V35 at 0,83*L*. Elongated LTs present. Abbreviations: DAC, dorsal anterior cone; DPC, dorsal posterior cone; ECT, epicentral tendon; ENT, epineural tendon; ENTB, epineural tendon bone; EPT, epipleural tendon; EPTB, epipleural tendon bone; F.NL, foramen for the *nervus lateralis*; HM, horizontal midline; LT, lateral tendon; MT, myorhabdoid tendon; RMA, attachment site of red musculature; RMTs, tendons within red muscle bundles; VAC, ventral anterior cone; VPC, ventral posterior cone

ENB/EPB—In the myosepta of V1–V7, an ENTB attaches to the neural arch (Figures 18d and 19a). It is unossified and tendinous (ENT) in the myosepta of V8–V19 (Figure 19b,c) and attaches to the middle of each neural spine (Figure 18a). In a few myosepta anterior to V20, an EPT attaches to the middle of each haemal spine (Figure 18a). An LT is present in all myosepta (Figures 18 and 19).

MT—There are no MTs anterior to V14 (Figure 19a). The anteriormost epaxial MT is present in the myoseptum of V14 and the

anteriormost hypaxial MT more posteriorly in the myoseptum of V18. The MTs reach their maximum length between V17 and V24 and become shorter again further posteriorly.

3.7.3 | Horizontal septum

Same as for *Astronesthes* except for the following: posterior to V8 (Figure 19), a short posterior oblique tendon (POT) connects a myoseptum to its succeeding centrum.

3.7.4 | Red musculature

Same as for *Astronesthes* except for the following that (1) the superficial red musculature covers the entire white musculature in all body regions (Figure 5f) and (2) The red muscle bundles medial to the superficial red musculature have only a single tendon at their connection to each myoseptum (Figures 18 and 19; RMT). It most likely represents the tendon of the dorsal muscle bundle.

3.7.5 | Caudal tendons

Same as for *S. elongatus* except for the following: The caudal tendons in *A. affinis* are LTs of the myosepta of V32–V35 (Figure 18c,d). Two MTs (most likely those of V34 and V35) insert on the dorsalmost caudal-fin rays, and only one on the ventralmost.

3.8 | Data analysis: Differences among species

For all the measurements, the 'Kruskal–Wallis tests' indicate significant differences among the investigated species (Table 3). The pairwise comparisons between the taxa also suggest significant differences across the investigated traits (LTep, lateral tendon epaxial; LThyp, lateral tendon hypaxial; MTep, myorhabdoid tendon epaxial; MThyp, myorhabdoid tendon hypaxial) (Figures 20–22). The comparisons among all species are summarized in Figure 20 and Table 5.

3.8.1 | *Astronesthes* sp.

In this species, the LTep is longer compared with most of the species. Only *S. elongatus*, *Polymetme* sp., and *A. affinis* show no significant differences compared with *Astronesthes* sp. regarding the length of LTep, MTep LThyp and MThyp. There are only slight differences compared with *C. sloani*. However, all tendons are comparatively longer than those of *E. simplex*, *E. obscurus* and *M. australis*.

3.8.2 | *Chauliodus sloani*

In this taxon, the majority of the measured traits are different compared with the rest of the species. The LTep displays consistent length differences that do not overlap with the other species. The length of the MTep in *C. sloani* is similar to that of *Astronesthes* sp., and *A. affinis*, while it differs significantly from the remaining taxa.

3.8.3 | *Eustomias simplex*, *E. obscurus*

Both *Eustomias* species are similar regarding their tendon lengths as summarized in the following. In the two *Eustomias* species, the LTep, MTep, LThyp and MThyp are short; in the pairwise comparison those traits differ from most of the species, and are most similar to *M. australis*.

3.8.4 | *Malacosteus australis*

The pairwise comparisons of the MTep show differences with most of the species, except the two *Eustomias* and *C. sloani*. The length of LTep, LThyp and MThyp differs from that of most of the species, with the exception of *E. simplex* and *E. obscurus*. In *Astronesthes* sp., *C. sloani*, *S. elongatus*, *Polymetme* sp. and *A. affinis* all tendons are longer.

3.8.5 | *Sigmops elongatus*

The tendons in this species are longer compared with the remaining taxa in this study. The pairwise comparisons also indicate significant differences of all investigated traits compared with the remaining taxa, except *Astronesthes* sp., *Polymetme* sp. and *A. affinis*. However, the MThyp is comparatively much shorter in *A. affinis*.

3.8.6 | *Polymetme* sp.

In this species, the tendons are longer than those of most of the investigated species (Table 6; Figure 20). The tendon lengths differ significantly to those of most of the species, except for *Astronesthes* sp. and *S. elongatus*. The epaxial tendons are similar in length to those of *A. affinis*.

3.8.7 | *Agryropelecus affinis*

The epaxial tendons (MTep, LTep) and LThyp are long and mostly similar to those of *Astronesthes* sp., *C. sloani*, *Polymetme* sp. and *S. elongatus*. The length of the MThyp in *A. affinis* differs from that of all the other species except *C. sloani*.

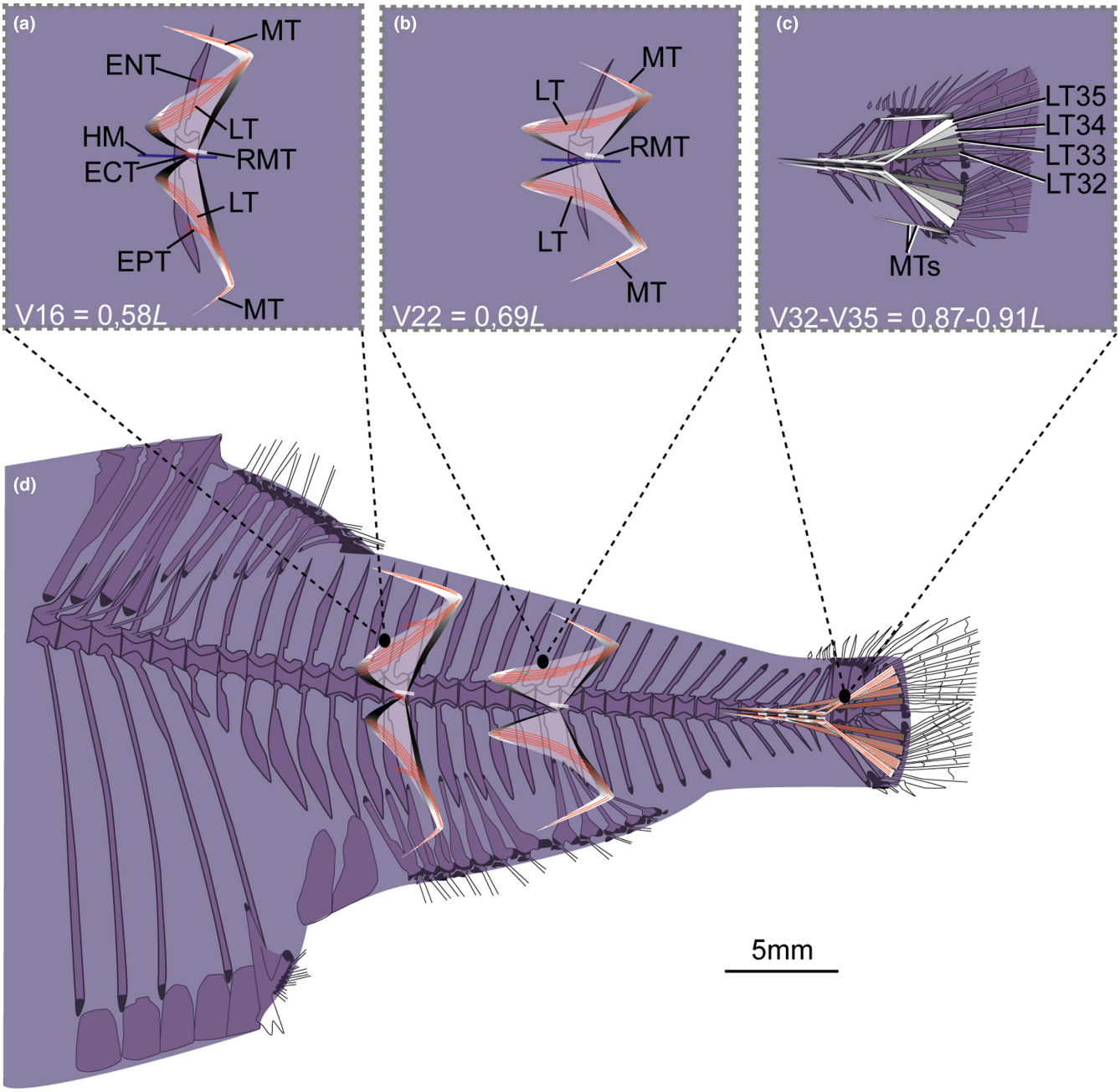

FIGURE 18 Schematic drawing of musculotendinous system (MTS) of different body regions in *Argyropelecus affinis* (MNHN 2021-0224, 59 mm SL). (a) Myoseptum of V16 at 0,58*L*. DAC/VAC present. ECT, LTs, ENT and EPT present. (b) Myoseptum of V22 at 0,69*L*. LTs extending from anterior into posterior cones. (c) Tendons that insert on caudal-fin rays and represent LTs of V32–V35. (d) Overview of different body regions and their MTS. Abbreviations: ECT, epicentral tendon; ENT, epineural tendon; EPT, epipleural tendon; HM, horizontal midline; LT, lateral tendon; MT, myorhabdoid tendon; RMT, tendon within red muscle bundles

3.8.8 | Differences among groups

For the comparisons between behavioural groups (migratory, non-migratory, semi-migratory, see Table 1), the 'Kruskal–Wallis test' indicates significant differences for all the measured traits (Table 4). The Wilcoxon pairwise comparisons between the groups indicate that in migratory species all tendons are longer compared with non-migratory species. Likewise, the semi-migratory group has longer tendons than the non-migratory (Table 6; Figure 21). However, tendon length is similar in the migratory and semi-migratory species. Given the striking short tendon lengths in *E. simplex*, *E. obscurus* in comparison to all other migratory species, we ran Wilcoxon pairwise comparisons excluding the two *Eustomias* species, and the results supports our statement that tendon lengths are longest in the migratory group and shortest in the non-migratory group with the semi-migratory group in between (Tables 7 and 8; Figure 22).

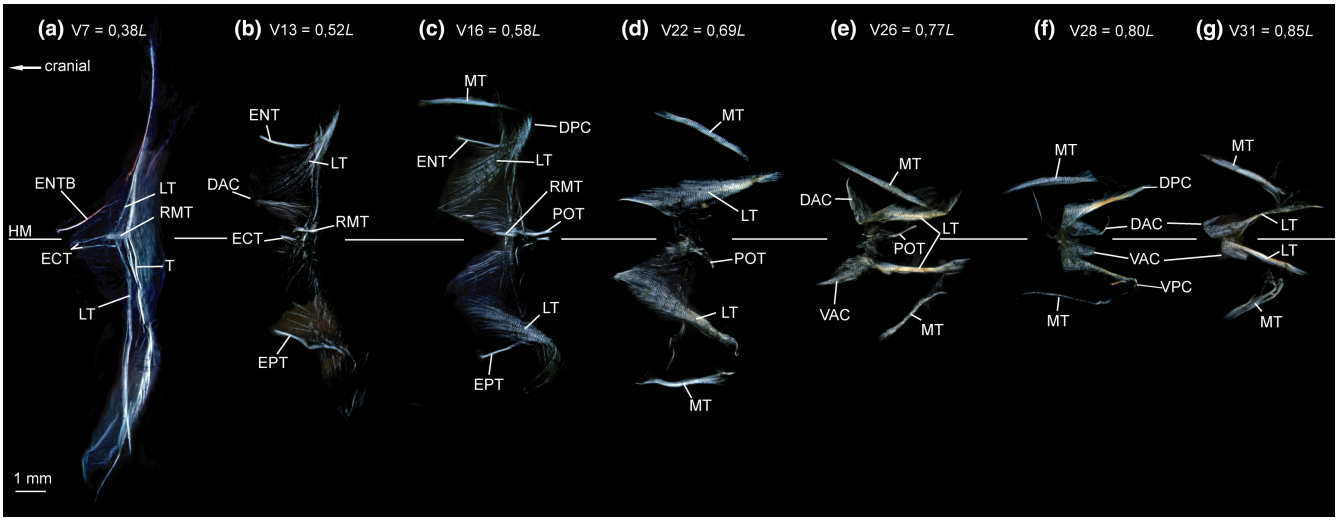

FIGURE 19 Dissected myosepta of *Argyropelecus affinis* (MNHN 2021-0224, 59 mm SL) photographed under polarized light. (a) Myoseptum of V7 at 0,38*L*. ECT, LTs and ENTB present. Posterior border of myoseptum tendinous (T). (b) Myoseptum of V13 at 0,52*L*. Anterior cones present. ECT, LTs, ENT and EPT present. (c) Myoseptum of V16 at 0,58*L*. As in (b) POT illustrated. (d) Myoseptum of V22 at 0,69*L*. LTs extending from anterior into posterior cones. (e) Myoseptum of V26 at 0,77*L*. Anterior cones elongated and turned dorsally/ventrally. (f) Myoseptum of V28 at 0,80*L*. DAC/VAC completely turned posteriad. (g) Myoseptum of V31 at 0,85*L*. DAC/VAC still turned posteriad, but not as much as in previous myosepta. Abbreviations: DAC, dorsal anterior cone; DPC, dorsal posterior cone; ECT, epicentral tendon; ENT, epineural tendon; ENTB, epineural tendon bone; EPT, epipleural tendon; HM, horizontal midline; LT, lateral tendon; MT, myorhabdoid tendon; POT, posterior oblique tendon; RMT, tendon within red muscle bundles; T, tendon at the posterior border of the myoseptum; VAC, ventral anterior cone; VPC, ventral posterior cone

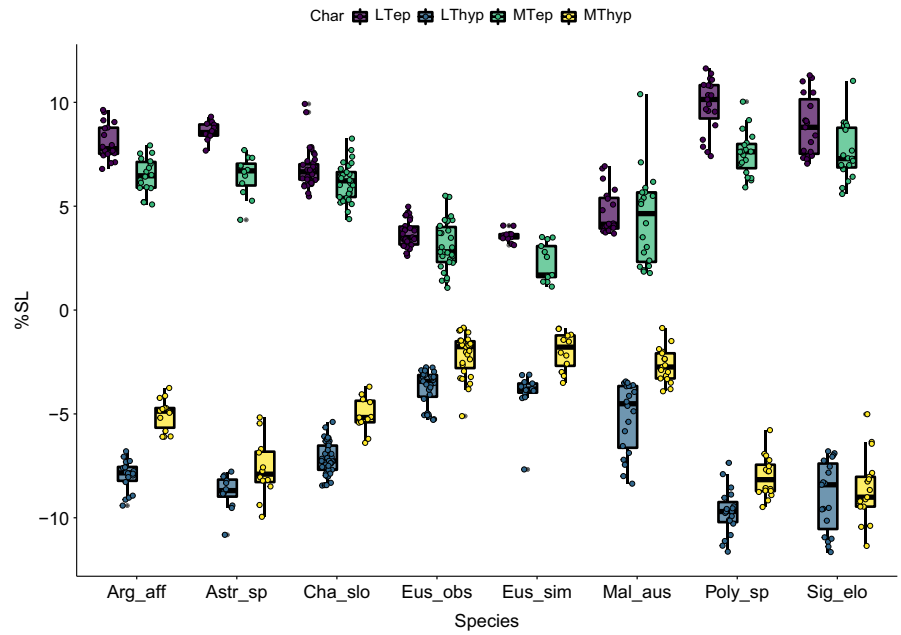

FIGURE 20 Boxplots of dispersion of traits for each of analysed species. Values indicated as percentage of standard length

3.9 | Data analysis: shared character states

Character 1: DAC of anteriormost myosepta: 0: small cones present, 1: without well–defined cones or cones absent.

Character 2: Myosepta with a HCS: 0: absent, 1: present.

Character 3: Myosepta increase in relative length towards the caudal fin through extreme elongation of the DAC and spans: 0: 1 centrum, 1: 2 centra, 2: 3.5 centra.

Character 4: DPCs: 0: not becoming shorter towards the caudal fin, 1: becoming shorter towards the caudal fin.

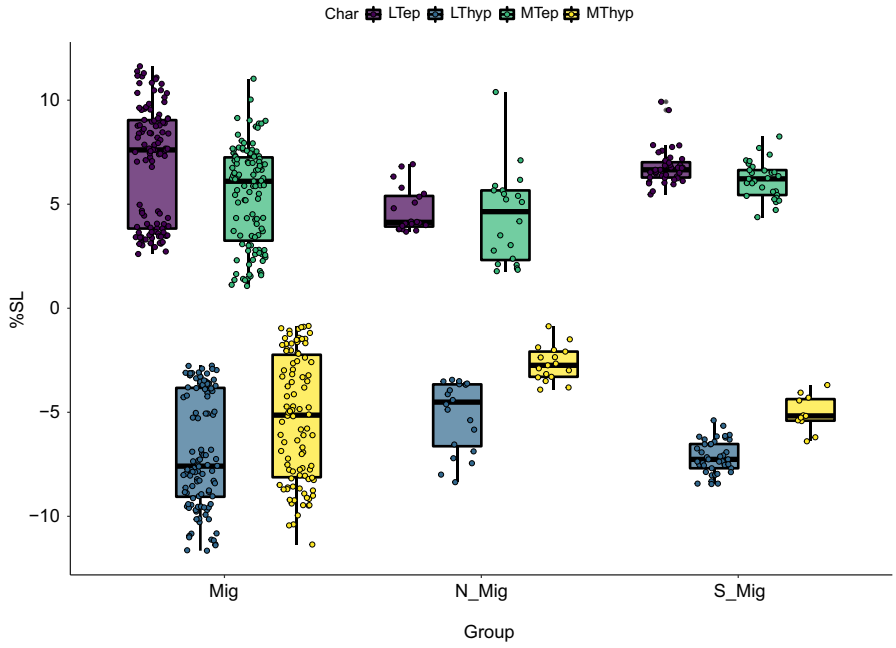

FIGURE 21 Boxplots of dispersion of traits for each of the three main groups. Values indicated as percentage of standard length. Mig = *Astronesthes* sp., *Eustomias obscurus*, *Eustomias simplex*, *Sigmops elongatus*; *Polymetme* sp., *Argyropelecus affinis*; S-Mig = *Chauliodus sloani*; Non-Mig = *Malacosteus australis*

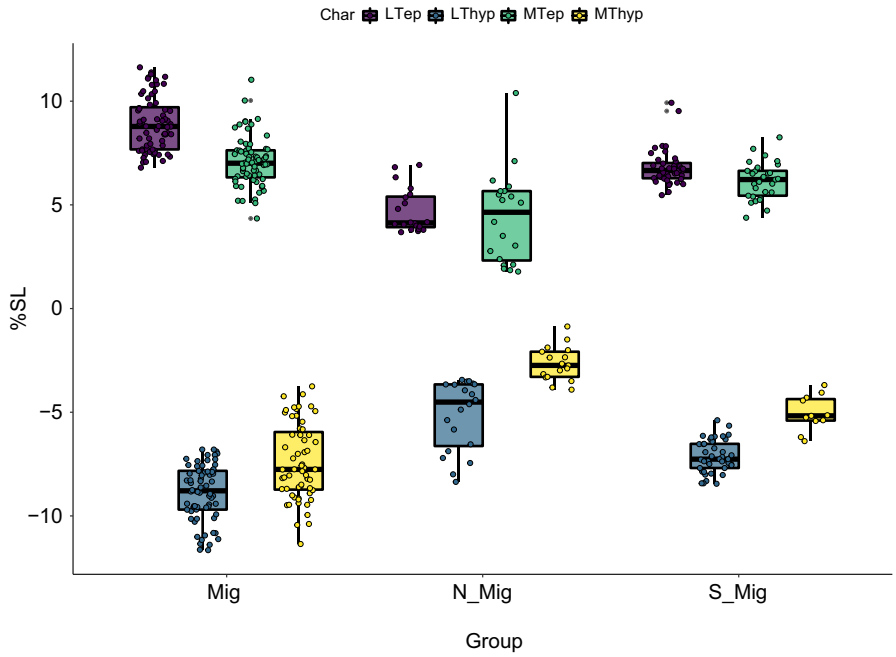

FIGURE 22 Boxplots of dispersion of traits for each of the three main groups excluding the two *Eustomias* species. Values indicated as percentage of standard length. Mig = *Astronesthes* sp., *Sigmops elongatus*; *Polymetme* sp., *Argyropelecus affinis*; S-Mig = *Chauliodus sloani*; Non-Mig = *Malacosteus australis*

Character 5: number of centra spanned by myosepta along body: 0: remains the same; 1: increases and then decreases again, 2: decreases and then increases again, 3: increases.

Character 6: ECT: 0: present, 1: absent.

Character 7: ECT of anteriormost myosepta: 0: inserted to the midline of the centrum, 1: inserted below the midline of the centrum.

Character 8: ECTs distally forked: 0: absent, 1: present.

Character 9: Anteriormost ECTs: 0: reach up to the passage for the *nervus lateralis*, 1: extend into the DPC.

Character 10: Posterior ENTs: 0: absent, 1: present.

Character 11: Four to six epineural bones forked proximally: 0: present, 1: absent.

Character 12: EPTBs: 0: present, 1: absent.

Character 13: Posterior EPTs: 0: absent, 1: present.

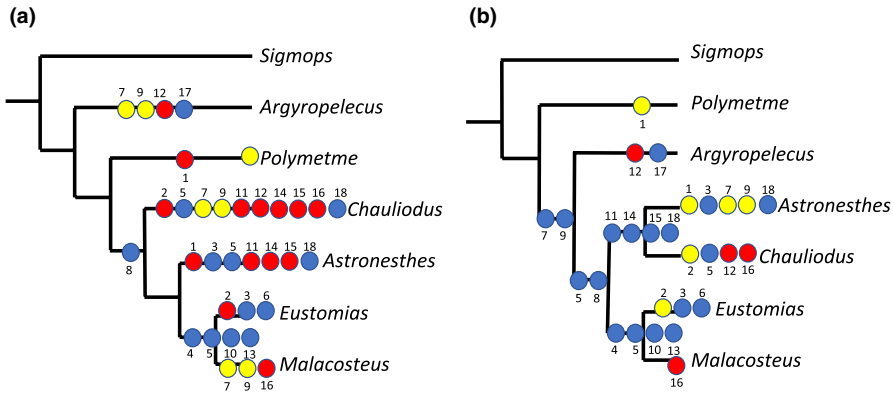

FIGURE 23 Tree comparisons. (a) Interrelationships of investigated taxa obtained by pruning the phylogenetic tree of Kenaley et al. (2013). We further mapped our characters on this tree (tree length: 33). (b) Single most parsimonious tree obtained from an exhaustive search performed using the data matrix given in Table 9 and rooted on *Sigmops elongatus* ($N = 1$, tree length 28, CI = 0.79, RI = 0.65). Blue circles, synapomorphies; red circles, convergences; yellow circles, reversals

Character 14: Four to six epipleural bones forked proximally: 0: present, 1: absent.

Character 15: LTBs: 0: absent, 1: present.

Character 16: VSAC: 0: absent, 1: present.

Character 17: Tendons in the two red muscle bundles dorsal and ventral to the horizontal midline that connect to the myoseptum are 0: paired, 1: single.

Character 18: number of caudal ligaments: 0: 4, 1: 3, 2: 7.

An exhaustive search for the most parsimonious hierarchy yielded a single tree of 28 steps, which is fully resolved, with a moderate level of homoplasy (CI = 0.79, RI = 0.65, see Figure 23b). In contrast to the pruned tree from Kenaley et al. (2013) (Figure 23a), *Argyropelecus* is sister to all stomiids united by state 0 of character 7 (ECT of anteriormost myosepta inserted to the midline of the centrum) and character 9 (anteriormost ECTs reach up to the passage for the *nervus lateralis*). Reversals in these two characters are found in *Astronesthes* sp. The stomiids *Astronesthes*, *Chauliodus*, *Eustomias* and *Malacosteus* are united by character 5 (number of centra spanned by myosepta along body: 0—remains the same; 1—increases and then decreases again, 2—decreases and then increases again, in contrast to character state 3—increases, found in the three non-stomiids) and character 8 (ECTs distally forked). *Astronesthes* and *Chauliodus* are united by characters 11 (four to six epineural bones forked proximally), character 14 (four to six epipleural bones forked proximally), character 15 (LTB's present) and 18 (number of caudal ligaments other than 4). *Eustomias* and *Malacosteus* are united by characters 4 (DPC's becoming shorter towards the caudal fin), character 5 (number of centra spanned by myosepta along body decreases and then increases again), character 10 (posterior ENTs absent) and character 13 (posterior EPTs absent) (Figure 23b).

4 | DISCUSSION

Locomotor diversity in fishes can be classified either by different swimming modes (anguilliform, carangiform, sub-carangiform, thunniform) depending on the amplitude of body undulation or by the 'body design' (maneuverer, accelerator, cruiser) in conjunction with hydrodynamics, modelling and ecology (Webb, 1984a, 1984b, 1988; Weihs, 1989; reviewed by Skafiotakis et al., 1999). In either case, locomotion in fishes is mainly driven by the three-dimensional structure of the MTS and the forces generated by muscle action transported via the MTS along the trunk (Gemballa, Ebmeyer, et al., 2003). Differences in the locomotion style are mirrored in anatomical differences in the MTS (e.g. Breder, 1926; Danos et al., 2008; Lindsey, 1978; Schwarz et al., 2012; Videler, 1993). In the following, the MTS of the investigated stomiiform species is discussed in correlation with their possible diel vertical migratory and feeding behaviour.

4.1 | Morphology of myosepta

4.1.1 | Anterior cones

In the anterior body region of all investigated stomiiform species, the myosepta have no anterior cones and attach right onto the anterior border of the respective centrum. Therewith, no anterior projection into the myomeric musculature exists in this body region. Only *Astronesthes* sp. and *Polymetme* sp. show tiny anterior projections most likely representing small anterior cones, slightly extending beyond the anterior border of the respective centrum in the anterior body region (Figures 2a and 16a).

The presence of anterior cones correlates with the presence of the dorsal fin on the body; however, the relative position of the dorsal fin differs in the investigated species. It is positioned far anteriorly in *C. sloani* (above V9: 18% body length) and *A. affinis* (above V8: 22% body length), at about midbody in *Astronesthes* sp. (above V25: 45% body length), *S. elongatus* (above V20: 50% body length), *Polymetme* sp. (above V15: 36% body length) and far caudally and opposed to the anal fin in *E. simplex* (above V45: 70% body length) and *M. australis* (above V33: 70% body length). In *Astronesthes* sp. and *Polymetme*

sp., the first anterior cones are present in those myosepta right in front of the dorsal-fin base. The DACs/VACs become clearly identifiable and anteriorly elongated in the succeeding myosepta (below the dorsal-fin base). In *E. simplex*, *M. australis*, *S. elongatus* and *A. affinis*, the DACs/VACs are present as of the myoseptum that is situated at the anterior end of the dorsal-fin base. In *C. sloani*, the DACs/VACs are present as of the myoseptum that is situated at the posterior end of the dorsal-fin base. There is a gradual anterior elongation of the anterior cones and together with the increase in density of the connective tissue in the myosepta; this indicates that the posterior most myosepta may be better equipped for a multisegmental force transmission towards the caudal fin (Gemballa & Röder, 2004).

4.1.2 | Posterior cones

The posterior cones project posteriorly into the myomeric musculature and span between one and four subsequent myomeres depending on body region and species. In the investigated specimens of *Astronesthes* sp., *S. elongatus*, *Polymete* sp. and *A. affinis*, the posterior cones span two to three subsequent centra. Posterior cone length in *Polymetme* sp. would support the observation of Cornejo and Koppelmann (2006) that it is a more active swimmer and possibly a migratory taxon contrary to the statement by Badcock (1984) that it is 'possibly non-migratory'. In *E. simplex* and *M. australis*, the posterior cones are, conversely, extremely short and only span one to one and a half subsequent centra. In *M. australis*, posterior cones become even shorter caudally and only span three quarters of a centrum. Extreme lengthening of the posterior cones is seen in *C. sloani*, where they span about four subsequent centra. In the primitive 'gnathostome condition', a myoseptum spans at least three subsequent centra (Gemballa, Ebmeyer, et al., 2003), which corresponds more or less to the length of the posterior projection of the posterior cones in stomiids, a condition also found in *Anguilla rostrata*, a catadromous migrator (Danos et al., 2008). In contrast, in *Carapus acus*, a highly flexible inquilinist that lives inside sea cucumbers, the posterior cones only span one centrum posteriorly (Schwarz et al., 2012).

4.1.3 | Relative length of entire myosepta

In stomiiforms, the myosepta span in rostrocaudal direction between 1.5 and 6.5 centra, depending on body region and species. The number of centra that the myosepta span throughout the body stays the same in *Astronesthes* sp. (about four). This number changes from anterior to posterior with more centra spanned posteriorly than anteriorly in *S. elongatus* and *A. affinis* (three centra anteriorly and five posteriorly), and in *Polymetme* sp. (four centra anteriorly and 6.5 posteriorly). Additionally, *Polymetme* sp. has the greatest relative length of myosepta or highest number of spanned centra of all studied taxa. In *C. sloani*, the myoseptum length is highest at mid-body where it is equal to the length of 5.5 centra, but shortens caudally again. The opposite is found in *E. simplex* and *M. australis* where myoseptum length is shortest at mid-body with a length of 1.5–2 centra. The myosepta elongate again caudally. Myoseptum lengths differ remarkably among specimens, the degree of elongation of myosepta in rostrocaudal direction correlates with body morphology and swimming mode. In non-carangiform swimmers, the maximum myoseptum length in the posterior body do not exceed the length of three centra, whereas in carangiform swimmers (e.g., *Scomber scombrus*) myoseptum lengths reach up to 4–6 centra lengths (Gemballa & Treiber, 2003; Shadwick & Gemballa, 2006). With maximum myoseptum lengths between 3 and 6.5 centra length, the investigated stomiiforms show myoseptum lengths that are somewhere in between those of non-carangiform and carangiform swimmers. Myoseptum lengths are greatest in thunniform swimmers like tunas, in which they span between 10 and 17 centra in the tail region (Donley et al., 2004; Ellerby et al., 2000; Fierstine & Walters, 1968; Kafuku, 1950; Katz, 2002; Knower et al., 1999; Nakae et al., 2014; Shadwick et al., 2002; Westneat et al., 1993; Westneat & Wainwright, 2001). It has been shown that in comparison with non-carangiform swimmers, the increase in myoseptal elongation over the length of the body is remarkable in carangiform and thunniform swimmers, ranging from anterior to posterior to up to 25% of the body length (Donley et al., 2004; Gemballa & Röder, 2004; Gemballa & Treiber, 2003; Shadwick & Gemballa, 2006). In contrast, the relative myoseptal length (in relation to length of centra), however, remains almost the same throughout the entire body in the investigated stomiiforms and, therefore, shows the pattern found in typical non-carangiform swimmers (Danos et al., 2008; Shadwick & Gemballa, 2006). The differences in myoseptum lengths found among the investigated species might correlate with their type of migratory behaviour: migratory, semi-migratory and non-migratory. This in turn would suggest that depth range of some species of e.g., *E. simplex* and *A. affinis* needs to be verified in further studies as information on their migratory behaviour is ambiguous in the literature and their MTS would suggest that *E. simplex* is a non-migratory (short relative length of myosepta) and *A. affinis* a migratory species (long relative length of myosepta) (Figures 20–22).

4.1.4 | Ventral secondary anterior cones

In some myosepta anterior to the anal fin, small VSACs are present in *C. sloani* and *M. australis*. VSACs have also been documented in the posterior body region in basal actinopterygians (polypterids, *Lepisosteus* and *Amia*) (Gemballa & Röder, 2004). In the latter taxa, they form additional tendons that attach to the caudal-fin rays. Additional data are needed in stomiiforms to address the possible function of VSACs during locomotion.

4.2 | Myoseptal tendons

Epineural/epipleural bone (can be either an ossification in the epineural/EPT, or the LT or a combination of both that then results in a forked ossification).

The highly conservative anatomy of myoseptal tendons in gnathostomes indicates that they play a prominent role in the force transmission framework in fishes (Gemballa, Ebmeyer, et al., 2003; Gemballa & Vogel, 2002; Shadwick & Gemballa, 2006). A single epineural and/or epipleural bone is present in each myoseptum anterior to the caudal region in all investigated taxa. In *Astronesthes* sp. and *C. sloani*, a few myosepta have a forked epineural/epipleural bone. Patterson and Johnson (1995, p. 28) found no proximal forkings in the epineural and epipleural bones in Stomiiformes, a character common in Salmoniformes. In contrast, we document here forking of epineural and epipleural bones in Stomiiformes, but only in a couple of myosepta in certain areas of the body. The anteromedial branch of these forked epineural/epipleural bones is an ossification of the epineural/EPT and usually attaches to the neural arch/parapophysis, whereas the anteroventral branch is an ossification in the LT and spans between the anterior and posterior cones. A forked epineural/epipleural bone is present in *Astronesthes* sp. and *C. sloani* in the first anteriorly elongated myoseptum with a noteworthy anterior cone below the dorsal fin base. Danos and Staab (2010) suggested that ossification of myoseptal tendons might occur when the myoseptal tendons experience even higher mechanical forces as a result of body form changes. In *Danio rerio*, proximal forking of the epineural is present at the precaudal–caudal transition (Bird & Mabee, 2003). In comparison to *Danio rerio*, proximal forking occurs further anteriorly in *Astronesthes* and *Chauliodus* and it remains to be established experimentally whether higher mechanical forces act in this area.

In all investigated genera, except *Astronesthes* sp. and *C. sloani*, the LT remains unossified along the trunk. The LT connects anterior and posterior cones. Values of myoseptal length reflect the length of the LT. An ossification in the LT is present in *Astronesthes* sp. and *C. sloani* in which it forms the anteroventral branch of the proximally forked epineural and/or epipleural bone. Further posteriorly in the body, there is no ossification in the epineural/EPT. The single ossification in the myoseptum is within the LT and connects anterior to posterior cone and thus the epineural/epipleural consists of just an LTB.

The LT is interrupted in *E. simplex* and *M. australis* with an anterior part running parallel to the horizontal septum and a posterior part reaching into the posterior cones. The LT that runs parallel to the horizontal midline might reinforce this region where the horizontal septum is reduced. Together with the tendons in the red muscle bundles the parallel LTs might effectively transmit muscle force to the caudal fin. As discussed under myoseptal length, the relative myoseptal length/LT length stays almost the same throughout the entire body in the here examined stomiiforms and, therefore, matches the pattern also found in non-carangiform swimmers (Shadwick & Gemballa, 2006). In contrast, in carangiform swimmers the LTs become significantly elongated towards the posterior region of the body.

To date the functional significance of tendons versus bones for a myoseptum has not been investigated. Gemballa and Treiber (2003) stated that the primitive set of three tendons within each epaxial myoseptum (MT, ENT, LT) contributes to its robustness. Two of these are myoseptal tendons that do not insert on skeletal or axial structures. In contrast, the ENT connects the neural arch with the skin. Gemballa and Treiber (2003) hypothesized that ENTs/EPTs minimize lateral backbone displacement during high body curvatures in non-carangiform swimmers based on their finding that these tendons are missing in posterior myosepta in *S. scombrus*, a carangiform swimmer that lacks high body curvatures. However, as experimental evidence is currently missing, we do not propose any functional explanation for the presence of myoseptal bones and their possible forked occurrence.

4.2.1 | Caudal tendons

In most taxa studied here, the last four myosepta are modified. They lack the posterior cone and mainly form posteriorly elongated LTs (four dorsal and four ventral LTs) that insert on caudal-fin rays. Two modified dorsal and ventral MTs, respectively, also insert on caudal-fin rays. Exceptions are *Astronesthes* sp. in which the seven last myosepta have 14 elongated LTs (seven epaxial tendons, seven hypaxial tendons) that insert on caudal-fin rays. In *C. sloani*, however, there are only three myosepta with elongated LTs, resulting in three epaxial tendons and three hypaxial tendons that insert on caudal-fin rays. The pattern of attachment is the same in all investigated taxa no matter if there are six or just four LTs and is as follows: The LTs of the last myoseptum insert dorsalmost/ventralmost on the caudal-fin rays, and the LTs of the anteriormost myoseptum, contributing to the caudal tendons, insert on the caudal-fin rays closest to the diastema (therewith close to the horizontal midline). The LTs in between insert progressively further dorsally or ventrally on caudal-fin rays. The muscle and tendinous system attaching to the caudal-fin rays has best been investigated in scombrids (Fierstine & Walters, 1968; Gemballa & Treiber, 2003; Westneat et al., 1993). There, the last five to six myosepta lack a posterior cone and form together the highly elongated great LT and the underlying medial caudal tendon attaching to caudal-fin rays. Direct force measurements in two tuna species have shown that red muscle forces are transmitted via those elongated caudal tendons (LT pathway) to the tail (Knower et al., 1999; Shadwick et al., 2002). However, experimental data on hydrodynamics and physiology are lacking for deep-sea fishes.

4.2.2 | Myorhabdoid tendons

The epaxial MTs in the investigated stomiiforms are strong in the anterior part of the body. They presumably transmit forces to the neurocranium, which can be elevated extremely during feeding, due to an occipito-vertebral gap (the lack or reduction of the anterior centra) and a functional head joint in some stomiid genera (Schnell et al., 2010; Schnell & Johnson, 2017). Future studies are necessary to evaluate whether this anatomical condition is linked with the size and appearance of the feeding apparatus. Shadwick and

Gemballa (2006) hypothesized that the MT and LT typically in gnathostomes spread out into horizontal fanlike tendons that project into the musculature. A similar anatomical condition was observed in the investigated stomiiform taxa. These horizontal fanlike tendons are very weak between adjacent cones of the anterior body, whereas in the posterior body they form mechanical links between adjacent cones (see also, Gemballa, Ebmeyer, et al., 2003; Gemballa & Treiber, 2003).

4.3 | Horizontal septum

Two different tendons can be distinguished within the horizontal septum, the ECTs and the POTs (Kafuku, 1950). The horizontal septum is reduced in almost all investigated stomiiforms, but it is distinct in the sternoptychids *A. affinis* and *A. olfersii*, the only investigated taxa with an oblique posterior tendon (POT) within the horizontal septum that connects the myosepta to the centra.

Epicentral tendons are present in the anterior body region of all examined taxa, except in *E. simplex* and are absent in those myosepta with more elongated anterior cones. They are distally forked in the investigated specimens of *Astronesthes* sp., *C. sloani* and *M. australis*. The dorsal branch of the distally forked epicentral tendon is very long in the anterior myosepta of *Astronesthes* sp. extending into the DPC. In contrast, the epicentral tendons are unbranched in *Polymetme* sp. and in the anterior body region of *S. elongatus*. In the latter species, however, the ECTs become paired further posteriorly, with one tendon dorsal to the horizontal midline and one ventral to it. In *A. affinis*, the epicentrals are short and paired, with one tendon dorsal and one ventral to the horizontal septum. The horizontal septum of gnathostomes, most comprehensively studied in scombrids, is hypothesized to play a role in swimming mechanics, transferring red muscle forces along tendon-like structures (POTs) to the vertebral axis (Westneat et al., 1993). Gemballa, Hagen, et al. (2003), nevertheless, showed that among fishes there is no unifying mechanism for the transfer of red muscle forces to the vertebral column via POTs or the HS. Shadwick and Gemballa (2006) suggested further study on this issue, as the red muscles do not directly insert on the POTs but rather on the myosepta.

It is most likely that the structures that transmit red muscle force to the vertebral column in stomiiforms investigated here are the tendons in the red muscle bundles probably replacing functionally the missing horizontal septum and POTs.

4.4 | Data analysis: differences between groups

The differences in characters among the taxa indicate that the migratory species display a wider range in the length of epaxial and hypaxial tendons than the other two groups (i.e. non-migratory and semi-migratory) (Tables 2 and 4). However, when the two *Eustomias* species are excluded, all measured structures are significantly longer in the migratory species compared with the non-migratory species, with the semi-migratory species in between (Tables 7 and 8; Figure 22).

Regarding the length of the epaxial and hypaxial tendons, semi-migratory taxa and non-migratory taxa show differences, with the semi-migratory taxa having relatively longer MTs and LTs. The migratory taxa do not show significant differences compared with the other two groups, unless the *Eustomias* species are excluded from the analyses (Table 6).

Further data on depth distributions during night and daytime for various stomiiform species are necessary to verify hypothesized behavioural patterns on their migratory capabilities based on the architecture of the MTS.

4.5 | Data analysis: relationships

We mapped our characters on the pruned phylogenetic tree based on molecular data from Kenaley et al. (2013) (Figure 23a) for comparison with our analysis (Figure 23b). Compared like this our analysis contains less evolutionary steps and reversals. We do not hypothesize that our analysis (Figure 23b) depicts the phylogenetic relationships of our studied taxa, but this tree was constructed for a heuristic purpose. We recover a monophyletic Stomiidae with *Chauliodus* and *Astronesthes* sister to each other and together sister to a clade that includes *Eustomias* and *Malacosteus* (Figure 23b). The placement of *Eustomias* within the 'Malacosteinae' has been proposed with molecular and morphological data (Kenaley et al., 2013; Schnell & Johnson, 2017). Further it has been documented that *M. niger* and *M. australis* are non-migratory species (Kenaley, 2007; Sutton & Hopkins, 1996), a fact that may correlate with the short posterior cones found in the taxa examined. This would also suggest that *E. simplex* that shows striking similarities of its MTS to *M. australis* is a non-migratory species, contradicting previous assumptions of its migratory behaviour (Sutton & Hopkins, 1996). With the data at hand, we cannot rule out that those shared similarities in the MTS of *E. simplex* and *M. australis* bear only a phylogenetic signal. Those similarities might also reflect adaptations to vertical migration. Our tree (Figure 23b) is to be seen as purely exploratory as the number of taxa and characters are not sufficient for a phylogenetic investigation. To elucidate stomiiform relationships, additional taxa from all four families are required as well as detailed morphological and phylogenetic analyses of the hypothesized sister taxon, the Osmeriformes (e.g. Betancur-R et al., 2017; Near et al., 2012; Straube et al., 2018).

4.6 | Red musculature

The body musculature of fishes unites red and white muscle segments composed of highly complexly arranged muscle fibres (Gemballa & Vogel, 2002; Shadwick & Gemballa, 2006). The nearly neutrally buoyant mesopelagic fishes have a muscular organization for sustained efforts that is of great significance for undertaking

vertical migrations (Marshall, 1971; Salvanes & Kristoffersen, 2001). It has been shown that the myomeres of mesopelagic fishes have an increase in the amount of red musculature towards the caudal fin (Marshall, 1971; Salvanes & Kristoffersen, 2001).

Red musculature is rich in fat, contains lots of glycogen, myoglobin, many mitochondria and is richly supplied with blood. These muscles are used for sustained slow swimming and gain their energy through the oxidation of fat. In contrast, white musculature serves as an emergency storage for fast movements, contains little or no fat, little glycogen, no myoglobin, few mitochondria and is more sparsely supplied with blood (Marshall, 1971). The stomiiforms investigated here have a substantial layer of subcutaneous red musculature around the white musculature, which increases in size towards the caudal region and covers the entire white musculature in the caudal peduncle. Only in *A. affinis* the white musculature of the entire body is covered with red musculature. Depth-related declines in metabolic rate, white muscle protein content and enzyme activities cause a reduction in routine locomotory activity, which is explained by the visual interactions hypothesis (VIH) (Childress, 1995; Drazen et al., 2013; Seibel & Drazen, 2007). As light levels decline with depth, the reactive distances between visually orienting predators and their prey are reduced and, therefore, the selective pressure for high-speed locomotion. As a result it is hypothesized that the relative amount of white muscles along the trunk is smaller in fishes of the pelagic, whereas the routine locomotory performance, and therefore the relative amount of red muscles, would generally remain the same regardless of light levels and depth (Drazen et al., 2013). However, this cannot be confirmed in the investigated taxa of stomiiforms. *Malacosteus australis* is a non-migrating species and shows less red musculature along the trunk than e.g., *Idiacanthus atlanticus* or even *A. affinis* (Figure 5c,e,f), as migratory species. The relative amount of white muscles in *Malacosteus* is higher than that in *Idiacanthus*, which could imply that *Malacosteus* is able to initiate fast starts after having spent time fairly motionless in the water column as a non-migrator.

The superficial red musculature that generally covers a significant part of the white musculature in the caudal region in mesopelagic fishes, including those investigated here, connects directly to the point in the myoseptum where the LT runs. Thus red muscle force transmission to the posterior cones and towards the caudal fin via the LTs seems possible and supports the proposed LT-pathway as force transmission mechanism in addition to/or instead of the POT-pathway (Gemballa & Treiber, 2003; Shadwick & Gemballa, 2006).

The red muscle bundles dorsal and ventral to the horizontal midline occupy an important space between the vertebral column and the outer superficial red musculature in the caudal region. In the precaudal region, these red muscle bundles are not internalized and lie subcutaneously. During this study, we demonstrated for the first time the presence of a tendon in each of the two red muscle bundles that attaches to the respective myoseptum. These tendons are distinct and well developed in the investigated stomiid species. In *S. elongatus*, the tendinous structure within the muscle bundles rather resembles an aponeurosis. In *Polymetme* sp., the tendons are short and only present in the caudal region, and in *A. affinis* there is only a single short tendon within the red muscle bundles.

In tunas and sharks, the internalized red musculature plays an important role in endothermy. There is an association between both thermal habitat and apparent endothermic capacity of two species of lamniform thresher sharks showing some form of endothermy (either red muscle endothermy or cranial endothermy) and entering the coolest water (Nakano et al., 2003; Sepulveda et al., 2005; Syme & Shadwick, 2011; Weng & Block, 2004). Future experimental studies measuring body temperature, however, are mandatory to confirm whether the internalized red muscle bundles in the caudal region in stomiids produce a level of endothermy and could play a role in stabilizing body temperature during DVMs and the related extreme changes in water temperature.

4.7 | Locomotion in stomiiformes

The topic of force transmission along the trunk of fishes is still controversially discussed. Either posterior muscle fibres serve as force transmitters that are active while being lengthened on the convex side of the body (e.g., in cruising species like *S. scombrus*) (Altringham & Ellerby, 1999; Gillis, 1998; Wardle et al., 1995), or this is achieved by myosepta with their longitudinally arranged tendons, e.g. the LT pathway, transmitting anteriorly generated forces to the tail (e.g. Gemballa, Ebmeyer, et al., 2003; Gemballa, Hagen, et al. 2003; Gemballa & Röder, 2004; Gemballa & Treiber, 2003). Additionally, muscle forces can be transmitted along the horizontal septum via ECTs (AOTs) and POTs as in tunas (Donley et al., 2004), but also along the skin with its surrounding scales if present (Gemballa & Röder, 2004).

Even though the investigated stomiiform species (*Astronesthes* sp., *C. sloani*, *E. simplex*, *M. australis*, *S. elongatus*, *Polymetme* sp., *A. affinis*) show an eel-like, elongated body form, the respective swimming style during steady swimming is not anguilliform (for explanation of anguilliform locomotion see e.g. Breder, 1926; Lauder & Tytell, 2005; Sfakiotakis et al., 1999). Rarely filmed encounters with stomiids show that the posterior part of the body undulates during steady swimming in synchronous waves (see e.g., https://www.mbari.org/products/creature-feature/pacific-viperfish/).

Thus, stomiiforms show rather a carangiform swimming mode, with stiff bodies and little lateral undulation during steady swimming. Lateral undulation is restricted to the caudal area. Webb (1975) previously stressed that one species might show more than just one swimming mode and a strict locomotion scheme should not be applied too rigorously. These rare encounters caught on video also show fast starts with large-amplitude body bending that results in high acceleration swimming manoeuvres. These are important components of a fish's locomotory repertoire to escape predators or to strike prey (Eaton et al., 1977; Wakeling, 2005). Even though the stomiiform swimming style during steady swimming rather resembles a carangiform more than an anguilliform swimming mode, their MTS corresponds to that described for anguilliform swimmers. Our

statistical analyses show that there is no fundamental difference in the myoseptum length/LT-length as postulated for carangiform swimmers (Shadwick & Gemballa, 2006). The anguilliform swimming mode might be reduced to tail propulsion during steady swimming to diminish the hydrodynamic disturbances in a relatively motionless deep-sea environment, thus conserving energy, but also reducing 'hydrodynamic noise' (water flow or turbulences). Stomiiforms and other deep-sea fishes have a relatively high number of superficial neuromasts that are directionally sensitive to water flows (Marranzino & Webb, 2018; Marshall, 1954, 1979, 1996; Marshall & Staiger, 1975) and more specifically detect flow velocity (Denton & Gray, 1989; Marranzino & Webb, 2018; McHenry & Liao, 2014).

5 | SUMMARY AND CONCLUDING REMARKS

Here we present detailed descriptions of the MTS and respective interpretations of the locomotion and vertical migration mode in mesopelagic fishes. We conclude that the 3D shape of the MTS varies from anterior to posterior in conjunction with the position of the dorsal fin. The anteriormost myosepta lack an anterior cone, whereas the posterior most myosepta lack a posterior cone. The latter have elongated LTs (the caudal tendons) that attach to the caudal-fin rays and transmit muscle forces from the body to the caudal fin. The morphology and the amount of red musculature that increases from anterior to posterior directly are related to this rostrocaudal force transmission. There are two different portions of red musculature, one that covers the white musculature laterally and two muscle bundles dorsal and ventral to the horizontal midline. Those muscle bundles lie subcutaneous in the anterior part of the body, but are internalized in the caudal region and occupy the space between the vertebral column and the skin in the horizontal plane. The relative amount of red musculature together with tendon lengths (LTs and MTs) possibly provides a first indication whether a certain mesopelagic species is a diel vertical migrator or a 'non-migrator'. Without physiological analyses, however, this correlation cannot fully be confirmed. Steady swimming (vertical or not) powered by red musculature seems essential in the mesopelagic zone to find prey, avoid predators and to reproduce.

ACKNOWLEDGEMENTS

The authors thank S. Raredon and J. Williams (USNM) for loan of specimens. Further they thank G. Carnevale for comments on an earlier version of this manuscript. For constructive comments and many helpful discussions during the project they are grateful to R. Britz (Senckenberg, Dresden), and D. Johnson (USNM). The latter two also served as reviewers and their comments greatly improved the manuscript. The authors have no conflict of interest to declare.

AUTHOR CONTRIBUTIONS

NS and CP designed the study, dissected the specimens, acquired the data and discussed the results. NS carried out the C&S, made the figures. CP and JK carried out the CT scan. FLR carried out the statistical analyses. NS and GL carried out the data matrix for the phylogenetic analyses. GL carried out the phylogenetic analyses and comparisons. All authors gave final approval to the ms.

DATA AVAILABILITY STATEMENT

The data that supports the findings of this study are available in the supplementary material of this article.

ORCID

Nalani K. Schnell https://orcid.org/0000-0003-2060-4656

REFERENCES

Alexander, R.M. (1967) *Functional design in fishes*. London: Hutchinson.

Alexander, R.M. (1969) The orientation of muscle fibers in the myomeres of fishes. *Journal of Marine Biological Association of the UK*, 49, 263–290.

Altringham, J.D. & Ellerby, D.J. (1999) Fish swimming: patterns in muscle function. *Journal of Experimental Biology*, 202, 3397–3403.

Badcock, J. (1970) The vertical distribution of mesopelagic fishes collected on the SOND cruise. *Journal of Marine Biological Association of the United Kingdom*, 50, 1004–1044.

Badcock, J. (1984) Gonostomatidae. In: Whitehead, P., Bauchot, M., Hureau, J., Nielsen, J. & Tortonese, E. (Eds.) *Fishes of the north-eastern Atlantic and the Mediterranean*, vol. I. Paris: UNESCO, pp. 284–301.

Bailey, D.M., Bagley, P.M., Jamieson, A.J., Collins, M.A. & Priede, I.G. (2003) In situ investigation of burst swimming and muscle performance in the deep-sea fish *Antimora rostrata* (Günther, 1878). *Journal of Experimental Marine Biology and Ecology*, 285–286, 295–311.

Bailey, D., Genard, B., Collins, M., Rees, J., Unsworth, S.K., Battle, E. et al. (2005) High swimming and metabolic activity in the deep-sea eel *Synaphobranchus kaupii* revealed by integrated in situ and in vitro measurements. *Physiological and Biochemical Zoology*, 78, 335–346.

Betancur-R, R., Wiley, O., Arratia, G., Acero, A., Bailly, N., Miya, M. et al. (2017) Phylogenetic classification of bony fishes. *BMC Evolutionary Biology*, 17, 162.

Bird, N.C. & Mabee, P.M. (2003) Developmental morphology of the axial skeleton of the zebrafish, *Danio rerio* (Ostariophysi: Cyprinidae). *Developmental Dynamics*, 228(3), 337–357.

Boddeke, R., Sljper, E.J. & Van de Stelt, A. (1959) Histological characteristics of the body-smusculature of fishes in connection with their mode of life. *Proceedings of the Koninklijke Nederlandse Akademie Von Wetenschappen. Amsterdam North Holland Publ. Co. Proceedings Series C: Biological and Medical Sciences*, 62, 576–588.

Breder, C.M. (1926) The locomotion in fishes. *Zoologica*, 4, 159–229.

Brierley, A.S. (2014) Diel vertical migration. *Current Biology*, 24(22), R1074–1076.

Britz, R. & Johnson, G.D. (2010) Occipito-vertebral fusion in actinopterygians: conjecture, myth and reality. Part 1: non-teleosts. In: Nelson, J.S., Schultze, H.-P. & Wilson, M.V.H. (Eds.) *Origin and phylogenetic interrelationships of teleosts*. München: Verlag Dr. Friedrich Pfeil, pp. 77–94.

Childress, J.J. (1995) Are there physiological and biochemical adaptations of metabolism in deep-sea animals? *Trends in Ecology and Evolution*, 10, 30–36.

Cornejo, R. & Koppelmann, R. (2006) Distribution patterns of mesopelagic fishes with special reference to *Vinciguerria lucetia* Garman 1899 (Phosichthyidae: Pisces) in the Humboldt Current Region off Peru. *Marine Biology*, 149, 1519–1537.

Danos, N., Fisch, N. & Gemballa, S. (2008) The musculotendinous system of an anguilliform swimmer: muscles, myosepta, dermis, and their interconnections in *Anguilla rostrata*. *Journal of Morphology*, 269, 29–44.

Danos, N. & Staab, K. (2010) Can mechanical forces be responsible for novel bone development and evolution in fishes. *Journal of Applied Ichthyology*, 26, 156–161.

Danos, N. & Ward, A.B. (2012) The homology and origins of intermuscular bones in fishes: phylogenetic or biomechanical determinants? *Biological Journal of the Linnean Society*, 106, 607–622.

Denton, E.J. & Gray, J.A.B. (1989) Some observations on the forces acting on neuromasts in fish lateral line canals. In: Coombs, S., Görner, P. & Münz, H. (Eds.) *Neurobiology and evolution: the mechanosensory lateral line*. New York: Springer, pp. 229–246.

Dingerkus, G. & Uhler, D.L. (1977) Enzyme clearing of Alcian blue stained whole small vertebrates for demonstration of cartilage. *Stain Technology*, 32, 229–231.

Domagk, G. (1933) Neuerungen auf dem Gebiet der histologischen Technik. *Medizin Und Technik*, 1, 126–136.

Donley, J.M., Sepulveda, C.A., Konstantinidis, P., Gemballa, S. & Shadwick, R.E. (2004) Convergent evolution in mechanical design of lamnid sharks and tunas. *Nature*, 429, 61–65.

Drazen, J.C., Dugan, B. & Friedman, J.R. (2013) Red muscle proportions and enzyme activities in deep-sea demersal fishes. *Journal of Fish Biology*, 83(6), 1592–1612.

Drazen, J.C. & Sutton, T.T. (2017) Dining in the deep: the feeding ecology of deep-sea fishes. *Annual Review of Marine Science*, 9, 337–366.

Eaton, R., Bombardieri, R.A. & Andmeyer, O.H. (1977) The Mauthner-initiated startle response in teleost fish. *Journal of Experimental Biology*, 66, 65–81.

Eduardo, L.N., Lucena-Frédou, F., Mincarone, M.M., Soares, A., Le Loc'h, F., Frédou, T. et al. (2020) Trophic ecology, habitat, and migratory behaviour of the viperfish *Chauliodus sloani* reveal a key mesopelagic player. *Scientific Reports*, 10(1), 20996.

Ellerby, D.J., Altringham, J.D., Williams, T. & Block, B.A. (2000) Slow muscle function of Pacific Bonito (*Sarda chilensis*) during steady swimming. *Journal of Experimental Biology*, 203, 2001–2013.

Fierstine, H.L. & Walters, V. (1968) Studies in locomotion and anatomy of scombroid fishes. *Memoirs of Southern Californian Academy of Sciences*, 6, 1–31.

Garnier, S. (2018) viridisLite: Default Color Maps from "matplotlib"(Lite Version). R package version 0.3.0.

Gemballa, S. & Britz, R. (1998) Homology of intermuscular bones in acanthomorph fishes. *American Museum Novitates*, 3241, 25.

Gemballa, S., Ebmeyer, L., Hagen, K., Hannich, T., Hoja, K., Rolf, M. et al. (2003) Evolutionary transformations of myoseptal tendons in gnathostomes. *Proceedings of the Royal Society B*, 270, 1229–1235.

Gemballa, S., Hagen, K., Röder, K., Rolf, M. & Treiber, K. (2003) Structure and evolution of the horizontal septum in vertebrates. *Journal of Evolutionary Biology*, 16, 966–975.

Gemballa, S., Konstantinidis, P., Donley, J.M., Sepulveda, C. & Shadwick, R.E. (2006) Evolution of high-performance swimming in sharks: transformations of the musculotendinous system from subcarangiform to thunniform swimmers. *Journal of Morphology*, 267, 477–493.

Gemballa, S. & Röder, K. (2004) From head to tail: the myoseptal system in basal actinopterygians. *Journal of Morphology*, 259, 155–171.

Gemballa, S. & Treiber, K. (2003) Cruising specialists and accelerators – are different types of fish locomotion driven by differently structured myosepta? *Zoology*, 106, 203–222.

Gemballa, S. & Vogel, F. (2002) Spatial arrangement of white muscle fibers and myoseptal tendons in fishes. *Comparative Biochemistry and Physiology*, 133A, 1013–1037.

Gillis, G.B. (1998) Neuromuscular control of anguilliform locomotion: patterns of red and white muscle activity during swimming in the American eel *Anguilla rostrata*. *Journal of Evolutionary Biology*, 201, 3245–3256.

Gray, J. (1933a) Studies in animal locomotion. I. The movement of fish with special reference to the eel. *Journal of Evolutionary Biology*, 10, 88–104.

Gray, J. (1933b) Studies in animal locomotion. II. The relationship between waves of muscular contraction and the propulsive mechanism of the eel. *Journal of Evolutionary Biology*, 10, 386–390.

Gray, J. (1933c) Studies in animal locomotion. III. The propulsive mechanism of the whiting (*Gadus merlangus*). *Journal of Evolutionary Biology*, 10, 391–400.

Gray, J. (1953) *The locomotion of fishes. Essays in Marine Biology*. Edinburgh: Oliver and Boyd, pp. 1–16.

Gray, J. (1968) *Animal locomotion*. New York: WW Norton & Co.

Johnson, G.D. & Britz, R. (2010) Occipito-vertebral fusion in actinopterygians: conjecture, myth and reality. Part 2: teleosts. In: Nelson, J.S., Schultze, H.-P. & Wilson, M.V.H. (Eds.) *Origin and phylogenetic interrelationships of teleosts*. München: Verlag Dr. Friedrich Pfeil, pp. 95–110.

Johnson, G.D. & Patterson, C. (2001) The intermuscular system of acanthomorph fishes: a commentary. *American Museum Novitates*, 3312, 1–24.

Kafuku, T. (1950) "Red muscles" in fishes. I. Comparative anatomy of the scombroid fishes of Japan. *Japan Journal of Ichthyology*, 1, 89–100. (in Japanese, English summary)

Katz, S.L. (2002) Design of heterothermic muscle in fish. *Journal of Experimental Biology*, 205, 2251–2266.

Kenaley, C.P. (2007) Revision of the stoplight loosejaw genus *Malacosteus* (Teleostei: Stomiidae: Malacosteinae), with description of a new species from the temperate southern hemisphere and Indian Ocean. *Copeia*, 886–900.

Kenaley, C.P., DeVaney, S.C. & Fjeran, T.T. (2013) The complex evolutionary history of seeing red: molecular phylogeny and the evolution of an adaptive visual system in deep-sea dragonfishes (Stomiiformes: Stomiidae). *Evolution*, 68–4, 996–1013.

Kinzer, J. & Schulz, K. (1988) Vertical distribution and feeding patterns of midwater fish in the central equatorial Atlantic II. Sternoptychidae. *Marine Biology*, 99, 261–269.

Knower, T., Shadwick, R.E., Katz, S.L., Graham, J.B. & Wardle, C.S. (1999) Red muscle activation pattern in yellowfin (*Thunnuns albacares*) and skipjack (*Katsuwonus pelamis*) tunis during steady swimming. *Journal of Experimental Biology*, 202, 2127–2138.

Lauder, G.V. (2015) Fish locomotion: recent advances and new directions. *Annual Review of Marine Science*, 7, 521–545.

Lauder, G.V. & Tytell, E.D. (2005) Hydrodynamics of undulatory propulsion. *Fish Biomechanics*, 23, 425–468.

Lindsey, C.C. (1978) Form, function, and locomotion in fish. *Fish Physiology*, 7, 1–100.

Marks, A., Kerstetter, D., Wyanski, D.M. & Sutton, T. (2020) Reproductive ecology of dragonfishes (Stomiiformes: Stomiidae) in the Gulf of Mexico. *Frontiers in Marine Science*, 7, 101.

Marrazino, A.N. & Webb, J.F. (2018) Flow sensing in the deep sea. The lateral line system of stomiiform fishes. *Zoological Journal of Linnean Society*, 183, 945–965.

Marshall, N.M. (1954) *Aspects of deep sea biology*, 1st edition. New York: Philosophical Library.

Marshall, N.B. (1971) *Exploration in the life of fishes*. Cambridge, MA: Harvard University Press.

Marshall, N.B. (1979) *Developments in deep sea biology*. Poole: Blandford Press.

Marshall, N.J. (1996) Vision and sensory physiology: the lateral line systems of three deep-sea fish. *Journal of Fish Biology*, 49(A), 239–258.

Marshall, N.B. & Staiger, J.C. (1975) Aspects of the structure, relationships, and biology of the deep-sea fish *Ipnops murrayi* (family Bathypteroidae). *Bulletin of Marine Science*, 25(1), 101–111.

Martin, A., Boyd, P., Buesseler, K., Cetinic, I., Claustre, H., Giering, S. et al. (2020) The oceans' twilight zone must be studied now, before it is too late. *Nature*, 580(7801), 26–28.

McHenry, M.J. & Liao, J.C. (2014) The hydrodynamics of flow stimuli. The Lateral Line, Springer Handbook of Auditory Research, 48.

Metscher, B.D. (2009) MicroCT for comparative morphology: simple staining methods allow high-contrast 3D imaging of diverse non-mineralized animal tissues. *BMC Physiology*, 9(11), 1–14.
Nakae, M., Sasaki, K., Shinohara, G., Okada, T. & Matsuura, K. (2014) Muscular system in the pacific bluefin tuna *Thunnus orientalis* (Teleostei: Scombridae). *Journal of Morphology*, 275, 217–229.
Nakano, H., Matsunaga, H., Okamoto, H. & Okazaki, M. (2003) Acoustic tracking of bigeye thresher shark *Alopias superciliosus* in the Eastern Pacific Ocean. *Marine Ecology Progress Series*, 265, 255–261.
Near, T., Eytan, R., Dornburg, A., Kuhn, K., Moore, J., Davis, M. et al. (2012) Resolution of ray-finned fish phylogeny and timing of diversification. *Proceedings of the National Academy of Sciences*, 109, 13698–13703.
Owen, R. (1846) *Lectures on the comparative anatomy and physiology of the vertebrate animals, part 1: fishes*. London: Longman, Greene.
Owen, R. (1866) *The anatomy of the vertebrates, Vol. 1: fishes and reptiles*. London: Longmans, Green.
Patterson, C. & Johnson, G.D. (1995) The intermuscular bones and ligaments of teleostean fishes. *Smithsonian Contributions to Zoology*, 559, 1–83.
R Core Team (2020) *R: A language and environment for statistical computing*. Vienna, Austria: R Foundation for Statistical Computing http://www.R-project.org/
Richards, T., Sutton, T.T. & Wells, R. (2020) Trophic structure and sources of variation influencing the stable isotope signatures of meso- and bathypelagic micronekton fishes. *Frontiers in Marine Science*, 7. https://doi.org/10.3389/fmars.2020.507992 507992.
Salvanes, A.G.V. & Kristoffersen, J.B. (2001) Mesopelagic fishes. *Encyclopaedia of ocean sciences*, vol. 3. New York: Academic, pp. 1711–1717.
Schnell, N.K., Britz, R. & Johnson, G.D. (2010) New insights into the complex structure and ontogeny of the occipito-vertebral gap in barbeled dragonfishes (Stomiidae, Teleostei). *Journal of Morphology*, 271, 1006–1022.
Schnell, N.K. & Johnson, G.D. (2017) Evolution of a functional head joint in deep sea fishes (Stomiidae). *PLoS One*, 12(2), e0170224.
Schwarz, C., Parmentier, E., Wiehr, S. & Gemballa, S. (2012) The locomotory system of pearlfish *Carapus acus*: what morphological features are characteristic for highly flexible fishes? *Journal of Morphology*, 273, 519–529.
Seibel, B.A. & Drazen, J.C. (2007) The rate of metabolism in marine animals: envi- ronmental constraints, ecological demands and energetic opportunities. *Philosophical Transactions of the Royal Society B*, 362, 2061–2078.
Sepulveda, C.A., Wegner, N.C., Bernal, D. & Graham, J.B. (2005) The red muscle morphology of the thresher sharks (family Alopiidae). *Journal of Experimental Biology*, 208, 4255–4261.
Shadwick, R.E. & Gemballa, S. (2006) Kinematics and muscle dynamics in undulatory swimming. *Fish Biomechanics. Fish Physiology*, vol. 23. San Diego, CA: Academic Press, pp 241–280.
Shadwick, R.E., Rapoport, H.S. & Fenger, J.M. (2002) Structure and function of tuna tail tendons. *Comparative Biochemistry and Physiology A*, 133, 1109–1125.
Skafiotakis, M., Lane, D. & Davies, J.B. (1999) Review of fish swimming modes for aquatic locomotion. *IEEE Journal of Oceanic Engineering*, 24, 237–252.
Straube, N., Li, C., Mertzen, M., Yuan, H. & Moritz, T. (2018) A phylogenomic approach to reconstruct interrelationships of main clupeocephalan lineages with a critical discussion of morphological apomorphies. *BMC Evolutionary Biology*, 18(1), 158.
Sutton, T.T. (2013) Vertical ecology of the pelagic ocean: classical patterns and new perspectives. *Journal of Fish Biology*, 83, 1508–1527.
Sutton, T.T. & Hopkins, T.L. (1996) Trophic ecology of the stomiid (Pisces: Stomiidae) fish assemblage of the eastern Gulf of Mexico: strategies, selectivity and impact of a top mesopelagic predator group. *Marine Biology*, 127, 179–192.
Sutton, T.T., Porteiro, F.M., Horne, J.K. & Anderson, C.I.H. (2010) Deep-pelagic fish interactions with seamounts and mid-ocean ridges. *Proceedings of an International symposium – into the unknown, researching mysterious deep-sea animals*. Okinawa: Okinawa Churaumi Aquarium, pp. 53–68.
Sward, D., Monk, J. & Barrett, N. (2019) A systematic review of remotely operated vehicle surveys for visually assessing fish assemblages. *Frontiers in Marine Science*, 6, 1–19.
Swofford, D.L. PAUP*: Phylogenetic Analysis Using Parsimony (*and Other Methods). Version 4.0. SinauerAssociates, Inc., 2002.
Syme, D.A. & Shadwick, R.E. (2011) Red muscle function in stiff-bodied swimmers: there and almost back again. *Philosophical Transactions of the Royal Society B*, 366, 1507–1515.
Taylor, W.R. & Van Dyke, G.C. (1985) Revised procedures for staining and clearing small fishes and other vertebrates for bone and cartilage study. *Cybium*, 9, 107–119.
Van Leeuwen, J.L. (1999) A mechanical analysis of myomere shape in fish. *Journal of Experimental Biology*, 202, 3405–3414.
Videler, J.J. (1993) *'Fish Swimming'*. London: Chapman and Hall.
Wainwright, S.A. (1983) To bend a fish. In: Shadwick, E.S. & Lauder, G.V. (Eds.) *Fish biomechanics*. New York: Praeger Publishers, pp. 68–91.
Wakeling, J.M. (2005) Fast-start mechanics. In: Shadwick, R.E. & Lauder, G.V. (Eds.) *Fish physiology*, vol. 23. San Diego, CA: Elsevier AcademicPress Inc., pp. 333–368.
Wardle, C.S., Videler, J.J. & Altrigham, J.D. (1995) Turning into fish swimming waves: body form, swimming mode and muscle function. *Journal of Experimental Biology*, 198, 1629–1636.
Webb, P.W. (1975) Hydrodynamics and energetics of fish propulsion. *Bulletin of the Fisheries Research Board of Canada*, 190, 1–159.
Webb, P.W. (1984a) Body form, locomotion, and foraging in aquatic vertebrates. *American Zoologist*, 29, 151–160.
Webb, P.W. (1984b) Form and function in swimming fish. *Scientific American*, 251, 58–68.
Webb, P.W. (1988) 'Steady' swimming kinematics of tiger musky, an esociform accelerator and rainbow trout, a generalist cruiser. *Journal of Experimental Biology*, 138, 51–69.
Weihs, D. (1989) Design feature and mechanics of axial locomotion in fish. *American Zoologist*, 29, 151–160.
Weng, K.C. & Block, B.A. (2004) Diel vertical migration of the bigeye thresher shark (*Alopias superciliosus*) a species possessing orbital retia mirabilia. *Fish*, 102, 221–229.
Westneat, M.W., Hoese, W., Pell, C.A. & Wainwright, S.A. (1993) The horizontal septum: mechanisms of force transfer in locomotion of scombrid fishes (Scombridae, Perciformes). *Journal of Morphology*, 217, 183–204.
Westneat, M.W. & Wainwright, S.A. (2001) Mechanical design for swimming: muscle, tendon, and bone. In: Block, B. & Stevens, E. (Eds.) *Fish physiology 19: tuna—physiology, ecology and evolution*. San Diego, CA: Academic Press, pp. 272–313.
Wickham, H. (2016) *ggplot2: elegant graphics for data analysis*. New York: Springer-Verlag.
Wienerroither, R., Uiblein, F., Bordes, F. & Moreno, T. (2009) Composition, distribution, and diversity of pelagic fishes around the Canary Islands, Eastern Central Atlantic. *Marine Biology Research*, 5, 328–344.
Woodstock, M.S. (2018) Trophic ecology and parasitism of a mesopelagic fish assemblage. Nova Southeastern University, Thesis.

SUPPORTING INFORMATION

Additional supporting information may be found in the online version of the article at the publisher's website.

How to cite this article: Schnell, N.K., Kriwet, J., López-Romero, F.A., Lecointre, G. & Pfaff, C. (2022) Musculotendinous system of mesopelagic fishes: Stomiiformes (Teleostei). *Journal of Anatomy*, 240, 1095–1126. Available from: https://doi.org/10.1111/joa.13614